https://doi.org/10.5194/hess-2019-638
Preprint. Discussion started: 23 January 2020

Hydrology and Earth System Sciences Discussions

Using hydrologic landscape classification and climatic time series to assess hydrologic vulnerability of the Western U.S. to climate

Chas E. Jones[1]*, Scott G. Leibowitz[2], Keith A. Sawicz[3], Randy L. Comeleo[2], Laurel E. Stratton[4], Phillip E. Morefield[5], Chris P. Weaver[6]

[1] Oak Ridge Institute for Science and Education (ORISE), c/o U.S. Environmental Protection Agency, Center for Public Health and Environmental Assessment, Pacific Ecological Systems Division, 200 SW 35th St., Corvallis, OR 97333, USA; Current affiliation: Affiliated Tribes of Northwest Indians, Corvallis, OR 97333, USA

[2] U.S. Environmental Protection Agency, Center for Public Health and Environmental Assessment, Pacific Ecological Systems Division, 200 SW 35th St., Corvallis, OR 97333, USA

[3] Oak Ridge Institute for Science and Education (ORISE), c/o U.S. Environmental Protection Agency, Center for Public Health and Environmental Assessment, Pacific Ecological Systems Division, 200 SW 35th St., Corvallis, OR 97333, USA

[4] c/o U.S. Environmental Protection Agency, Center for Public Health and Environmental Assessment, Pacific Ecological Systems Division, 200 SW 35th St., Corvallis, OR 97333, USA

[5] U.S. Environmental Protection Agency, Center for Public Health and Environmental Assessment, Health and Environmental Effects Assessment Division, Washington, DC 20460, USA

[6] U.S. Environmental Protection Agency, Center for Public Health and Environmental Assessment, Health and Environmental Effects Assessment Division, Research Triangle Park, NC 27709, USA

Correspondence to: Chas E. Jones (chas@chasjones.com)

https://doi.org/10.5194/hess-2019-638
Preprint. Discussion started: 23 January 2020

Hydrology and Earth System Sciences
Discussions

Abstract. We apply the hydrologic landscapes (HL) concept to assess the hydrologic vulnerability of the western United States (U.S.) to projected climate conditions. Our goal is to understand the potential impacts for stakeholder-defined interests across large geographic areas. The basic assumption of the HL approach is that catchments that share similar physical and climatic characteristics are expected to have similar hydrologic characteristics. We map climate vulnerability by integrating the HL approach into a retrospective analysis of historical data to assess variability in future climate projections and hydrology, which includes temperature, precipitation, potential evapotranspiration, snow accumulation, climatic moisture, surplus water, and seasonality of water surplus. Projections that are not within two-standard deviations of the historical decadal average contribute to the vulnerability index for each metric. This allows stakeholders and/or water resource managers to understand the potential impacts of future conditions. In this paper, we present example assessments of hydrologic vulnerability of specific geographic locations (Sonoma Valley, Willamette Valley, and Mount Hood) that are important to the ski and wine industries to illustrate how our approach might be used by specific stakeholders. The resulting vulnerability maps show that temperature and potential evapotranspiration are consistently projected to have high vulnerability indices for the western U.S. Precipitation vulnerability is not as spatially uniform as temperature. The highest elevation areas with snow are projected to experience significant changes in snow accumulation. The seasonality vulnerability map shows that specific mountainous areas in the West are most prone to changes in seasonality, whereas many transitional terrains are moderately susceptible. This paper illustrates how the HL approach can help assess climatic and hydrologic vulnerability across large spatial scales. By combining the HL concept and climate vulnerability analyses, we provide a planning approach that could allow resource managers to consider how future climate conditions may impact important economic and conservation resources.

1 Introduction

A stable and predictable water supply is imperative to national security (National Intelligence Council, 2012), especially as it pertains to the global food supply, and the threats of increased flooding, droughts, wildfire, and more extreme temperatures (Mancosu et al., 2015; Mekonnen and Hoekstra, 2016). The recognition of the potential threats of climate on society is important, and the development of planning tools could help decision-makers assess the risk imposed by projected environmental changes, such as those imposed by climate, population growth, or habitat conversion (Glick et al., 2011; Lawler et al., 2010). Environmental changes related to climate and hydrology will not impact stakeholders equally across sectors, thus the specific concerns and adaptation strategies of different industries will vary.

Numerous studies have examined projected changes in climate and hydrology on regional and national scales that included the western U.S. The Third National Climate Assessment (http://nca2014.globalchange.gov) is a comprehensive resource for climate-related research in the U.S. (Melillo et al., 2014). Nolin and Daly (2006) mapped climate-related risk to snow-dominated areas and ski areas in the Pacific Northwest. Mote et al. (2005) compared the spatial patterns of snow water equivalent observations to model simulations in the western U.S. Brown and Mote (2009) examined projected changes in snow water equivalent globally based on 14 model projections. Barnett et al. (2005) identified potential climate-driven water supply deficits in snow-dominated areas around the globe, although rising water demands have been found to greatly outweigh potential climate impacts on future (year 2025) water

https://doi.org/10.5194/hess-2019-638
Preprint. Discussion started: 23 January 2020

supply (Vorosmarty et al., 2000). McAfee (2013) examined projected changes in potential evapotranspiration (PET, calculated using numerous methods) between 2002-2011 and 2079-2098. The findings are consistent across studies in many areas of the globe including across the conterminous U.S., but other regional PET predictions were inconsistent and sensitive to the method of calculation. Hill et al. (2013, 2014) predicted thermal vulnerability of streams and river ecosystems to climate across the U.S., while Battin et al. (2007) found that in regards to salmon habitat, snow-dominated streams were more vulnerable habitat than lowland streams. The analyses of Nijssen et al. (2001) on hydrologic sensitivity of rivers globally found: 1) Ubiquitous warming, with greatest warming in winter months at higher latitudes, 2) More precipitation with high variability, 3) Early to mid-spring snowmelt caused increased spring streamflow peak in coldest basins, decreased spring runoff and increased winter runoff in transitional basins, 4) Tropical or mid-latitude basins had decreased annual runoff, and 5) High latitude basins had increased annual streamflow. In response to droughts of the recent past, Mann and Gleick (2015) highlight the strong correlation between very hot years and very dry years; thus as temperatures increase, precipitation is becoming more scarce. A study by Cook et al. (2015) found a growing risk of unprecedented drought in the western U.S. based on temperature projections and no clear pattern in future precipitation.

“Vulnerability” has many accepted definitions depending upon discipline and application (Adger, 2006; Füssel, 2007). Vulnerability assessments often integrate exposure, sensitivity, and adaptive capacity to stressors (Adger, 2006; Füssel, 2007; Füssel and Klein, 2006; IPCC, 2014). Researchers have studied vulnerability at varying scales across numerous regions for a diversity of stakeholders, and they tend to focus on the most relevant metrics for their particular application (Farley et al., 2011; Glick et al., 2011; IPCC, 2014; Nolin and Daly, 2006; U.S. Global Change Research Program, 2011; Watson et al., 2013). Yet, better products and services are needed to enable local communities to plan for and respond to hydrologic change, which includes services that improve understanding, observing, forecasting, and warning about significant hydrologic events (Tansel, 2013). Glick et al. (2011) and Lawler et al. (2010) both emphasize the importance to managers of understanding the potential impacts of climate on the resources that they manage.

There have been many efforts to assess hydrologic vulnerability related to specific stakeholders, ecosystems, or locations. For example, Vörösmarty et al. (2000) examined the vulnerability of global water resources to changes in climate and population growth. Hill et al. (2014) assessed stream temperature vulnerability to climate for sites across the U.S. In another example, Winter (2000) suggested that the vulnerability of wetlands to changes in climate depends upon their position within the hydrologic landscape.

There are opportunities to build upon previous efforts to map hydrologic vulnerability across large geographic areas, while creating tools that stakeholders may use to understand the potential impacts for their asset of interest in specific watersheds. Winter (2001) described the concept of classifying the physical landscape and climatic properties of catchments based on hydrologic landscapes (HL). Surface and ground water availability in watersheds is impacted by differences in geology, terrain, soils, seasonal temperature patterns, precipitation magnitude, and precipitation timing (Tague et al., 2013; Winter, 2001) and are not uniform across regions (Hamlet, 2011; Jung and Chang, 2012; Tague and Grant, 2004). Catchments that share similar key physical and climatic characteristics are expected to have similar hydrologic characteristics; i.e., surface and ground water interactions, deposition, timing, and accumulation of precipitation, surface runoff patterns, and groundwater flow (Nolin, 2011; Thompson and Wallace, 2001).

The HL concept has been applied to the U.S. (Wolock et al., 2004) and modified approaches have been used in Oregon (Leibowitz et al., 2014; Patil et al., 2014; Wigington et al., 2013), Nevada (Maurer et al., 2004), the Pacific Northwest (Comeleo et al., 2014; Leibowitz et al., 2016), and Bristol Bay, Alaska (Todd et al., 2017). In applying the HL approach in Oregon and the Pacific Northwest, two climatic factors and three landscape characteristics were categorized for each catchment; the resulting classification allows the prediction of catchment-scale hydrologic behavior across large spatial scales. The approach shows promise in predicting seasonal and monthly hydrologic patterns (Leibowitz et al., 2014). Leibowitz et al. (2014) adapted the classification system applied by Wigington et al. (2013) to illustrate the applicability of HLs for representing normal (1971-2000) monthly average streamflow in three case study watersheds in Oregon. They used climate projections (2041-2070) to estimate hydrologic behavior of catchments relative to 1971-2000. Leibowitz et al. (2016) expanded the approach and applied the HL classification to Oregon, Washington, and Idaho.

A number of tactics have been used to investigate the influence of climate on hydrologic behavior (Luce and Holden, 2009; Safeeq et al., 2014; Vano et al., 2015). To extend the work previously completed from HL-based climate projections, we assess climate vulnerability at the catchment scale by integrating the HL approach into an analysis of climatic variability. Our hydrologic landscape vulnerability analysis (HLVA) provides spatially continuous, application-specific estimates of climatic vulnerability. One of the benefits of the HLVA is to place modern and projected environmental changes in the context of available historic data. In the HLVA, we use proxies for the three components of vulnerability: a) historic climate data and their derivatives as proxies for sensitivity; b) climate projections as proxies for exposure; and c) qualitative considerations of ecosystems, stakeholders, or industries as proxies for adaptive capacity. The HLVA assesses vulnerability to changes in temperature, precipitation, potential evapotranspiration, snow accumulation, climatic moisture, surplus water, and seasonality of the water surplus. This method highlights areas that are projected to experience deviations from historic conditions to understand the patterns in magnitude, timing, and type of precipitation and the quantity and seasonality of available water at a catchment scale.

We apply the HL concept with the goal of assessing the hydrologic vulnerability of the western U.S. to magnitude and variability in climate projections. We analyzed this data to address three research objectives: 1) develop an index of vulnerability based on past and projected climate behavior; 2) map areas that are projected to be more vulnerable to environmental changes associated with climate; and 3) determine the vulnerability indices of seven metrics (temperature, precipitation, snow accumulation, PET, surplus water (S'), Feddema Moisture Index (FMI; Feddema, 2005), and seasonality) for specific geographic areas, including three examples of industries that are economically important in the region.

2 Methods

2.1 Study Area

https://doi.org/10.5194/hess-2019-638
Preprint. Discussion started: 23 January 2020

Hydrology and Earth System Sciences
Discussions

The study area includes the states of Washington, Oregon, Idaho, California, Nevada, and Arizona in the western U.S. (Fig. 1). These states extend across a wide range of climates and diverse physiographic settings. The lowest elevation across the six states is 85 m below sea level (Death Valley, California), while the highest elevation is 4421 m above sea level (Mt. Whitney, California) [U.S.G.S. National Elevation Dataset available at: https://nationalmap.gov/elevation.html]. The Sierra-Nevada Mountains are oriented in a north-south direction near the eastern border of California and transition to the Cascade mountain range that runs in a north/south direction through Oregon and Washington. (US Topo Quadrangles available at: https://nationalmap.gov/ustopo). However, there are numerous mountain ranges in each of the other states as well. The Sierra-Nevada and Cascade mountain ranges generate orographic effects that cause upwind areas to the west to have much greater precipitation relative to the downwind, eastern regions (Dettinger et al., 2004; Siler et al., 2013). High elevation areas receive most of their precipitation as snow (Brekke et al., 2009; Mote et al., 2005), while lowland and coastal areas receive their precipitation mostly as rain (Brekke et al., 2009; Mock, 1996), but much of the six-state area receives a balance of snow and rain. The topographic differences across the landscape drive precipitation patterns across the six state study area and cause large differences in the total annual precipitation or the seasonality of maximum precipitation (Mock, 1996). In the arid southwest, summer monsoons deliver most of the annual precipitation (Mock, 1996), whereas in the Pacific Northwest, winter rains and snows are the dominant form of precipitation (Mock, 1996). However, the western U.S. is regularly affected by atmospheric rivers that deliver large quantities of rain or snow over short periods (Dettinger, 2011; Hidalgo et al., 2009). The seasonal variability of surface air temperature varies widely across the study area. Portions of each state in our study area are classified as deserts with summer maximum temperatures regularly exceeding 40°C (NOAA State Climate Extremes Committee, 2016). Each state in the study area has also recorded temperatures less than -40°C (NOAA State Climate Extremes Committee, 2016). Some portions of the study area have very mild climates with little seasonal variation in temperature (Daly, 2016b). Bedrock geology in the study area varies from high permeability sedimentary deposits or relatively recent volcanic deposits, to low permeability igneous metamorphic and sedimentary formations and older volcanics (Comeleo et al., 2014; Stratton et al., 2016).

2.2 Hydrologic landscape classification

The study area was divided into 29,356 assessment units (AUs). The AUs are aggregations of NHDPlusV2 catchments (McKay et al., 2012) that were grouped to have a target area of 80 km^2, as described in Wigington et al. (2013) and modified by Leibowitz et al. (2016). For this analysis, we retain an AU if its centroid was located within the boundary of our project area or if the AU extended across an international boundary. All AU polygons are also clipped to the international boundary of the U.S. These conditions allow us to avoid edge effects at international and state borders by avoiding overlapping AUs at state boundaries and analyzing the HLs up to all international borders. The project boundary was defined by merging these AUs into a single polygon.

Wigington et al. (2013) developed their HL classification based on climatic and physical characteristics of the physical watershed. They defined five indices to characterize the major drivers that control the magnitude and timing of water movement through the landscape and into the ground or stream network: (1) climate, which describes the overall availability of water on the landscape, (2) seasonality of water surplus, which is the season when the maximum excess of water is available to infiltrate into the soil column or flow as surficial runoff, (3) subsurface permeability, (4) terrain,

https://doi.org/10.5194/hess-2019-638
Preprint. Discussion started: 23 January 2020

and (5) surface permeability. Note that Wigington et al. (2013) referred to subsurface and surface permeability as aquifer and soil permeability, respectively. The five HL indices, described in more detail below (Sections 2.2.1 through 2.2.5), are typically concatenated into a 5-character HL code (e.g., WsLMH, SwHTH, or DfHfL) that characterizes an AU.

Leibowitz et al. (2016) developed an HL map of the Pacific Northwest (PNW, consisting of Oregon, Idaho, and Washington) based on a modification of the Wigington et al. (2013) approach (herein described as the modified Wigington et al. (2013) approach). For the current effort, we used the modified Wigington et al. (2013) approach to develop an HL classification of California, Nevada, and Arizona [referred to as the southwest]. This was then combined with the PNW map (Leibowitz et al., 2016) to create an HL map of the six western states.

2.2.1 Climate

The Wigington et al. (2013) approach derived the climate index from the FMI (Feddema, 2005):

$$FMI = \begin{cases} 1 - \frac{PET}{P} & if\ P \geq PET \\ \frac{P}{PET} - 1 & if\ P < PET \end{cases} \tag{1}$$

where FMI (Eq. (1)) values range from -1.0 (arid) to 1.0 (very wet). P is the mean precipitation (mm) over a 30-year normal, which is derived from climate data described in Section 2.3, and PET is the potential evapotranspiration (mm) calculated using the Hamon (1961) method, that utilizes mean daily temperature, daytime length (calculated based on latitude), and a calibration coefficient. The range of FMI values was the basis for a climate index consisting of six classes: arid (A; $-1.0 \leq FMI < -0.66$), semiarid (S; $-0.66 \leq FMI < -0.33$), dry (D; $-0.33 \leq FMI < 0.0$), moist (M; $0.0 \leq FMI < 0.33$), wet (W; $0.33 \leq FMI < 0.66$), and very wet (V; $0.66 \leq FMI < 1.0$) (Wigington et al., 2013). FMI was calculated from regional precipitation rasters (described in Section 2.3) for each period of interest. The FMI value was then averaged over each AU.

2.2.2 Seasonality

We used the Leibowitz et al. (2016) approach to develop a seasonality index that identifies the season of the maximum monthly average snowpack-corrected surplus water (S'_m):

$$\begin{aligned} S'_m &= S_m - \Delta PACK^*_m \\ &= (P_m - PET_m) - (PACK^*_m - PACK^*_{m-1}) \end{aligned} \tag{2}$$

where S'_m (Eq. (2)) is the average snowpack-corrected water surplus (mm) for month *m*, S_m is monthly water surplus (P - PET), and P_m and PET_m are monthly precipitation and monthly PET, respectively. $PACK_m^*$ is a monthly bias-corrected snowpack value (in mm of snow water equivalent, or SWE) restricted to values greater than zero, based on the Leibowitz et al. (2016) modifications to the Leibowitz et al. (2012) snowpack model. Note, however, that $\Delta PACK^*_m$ can have negative values, which represents snow melt. For each month, S'_m was calculated for the regional raster, before identifying the month of maximum S'_m for the majority of pixels in each AU. The month of maximum S'_m was used to identify the season of maximum S'_m based upon four seasonality classes: fall (f; October–December), winter (w; January–March), spring (s; April–June), and summer (u; July–September). The PNW analysis by Leibowitz et al. (2016) only included two seasonality classes; summer seasonality did not occur, while fall and winter were combined into a winter class, since this represented the PNW's wet season. For our analysis, we kept winter and

https://doi.org/10.5194/hess-2019-638
Preprint. Discussion started: 23 January 2020

fall separate and used all four seasonality classes, because fall and winter are distinct seasons in other parts of the nation.

2.2.3 Subsurface permeability

Leibowitz et al. (2016) utilized the Comeleo (2014) aquifer permeability dataset. We applied a similar approach from the Stratton et al. (2016) aquifer permeability datasets, which is herein referred to as subsurface permeability. Each of these datasets classify the subsurface permeability into high (H) and low permeability (L) classes, which are assigned with a threshold guideline of 8.5 x 10^{-2} m day^{-1} hydraulic conductivity. Using these data, we analyzed the subsurface permeability of each AU by identifying the subsurface permeability class for the majority of pixels within each AU in the three south western states.

2.2.4 Terrain

To classify terrain, we used the same approach as Wigington et al. (2013). We analyzed a 30 m Digital Elevation Model to classify the landscape based upon the topographic characteristics of each AU. "Mountainous" (M) areas had AUs with <10 % of the area identified as flat (< 1 % slope) and greater than 300 m of total relief. AUs with more than 50 % area having < 1 % slope were classified as "flat" (F). All other AUs were identified as "transitional" (T).

2.2.5 Surface permeability

For surface permeability, the Wigington et al. (2013) HL approach utilized the STATSGO soil permeability raster developed by Pennsylvania State University Center for Environmental Informatics (www.cei.psu.edu) for the top 10 cm of soil (Miller and White, 1998) in the conterminous U.S. The STATSGO soils database was selected because of its complete coverage of the conterminous U.S., despite SSURGO's higher spatial resolution, which did not have complete spatial coverage of the U.S. They identified whether the majority of each AU had high (H; >1.52 cm/hr) or low (L; ≤ 1.52 cm h^{-1}) soil permeability. We applied the same approach to classify surface permeability of each AU into two classes throughout the region.

2.3 Climate analyses

2.3.1 Modern climate normal (1971−2000)

Average monthly precipitation and mean temperature were acquired from Parameter-elevation Regressions on Independent Slopes Model (PRISM; Daly, 2016b) data for our normal climatic period at a resolution of approximately 400 m. The PRISM Climate Mapping Program is an ongoing effort to produce detailed, spatial climate datasets (Daly, 2016a; Daly et al., 2000). PRISM uses point measurements of climate data and a digital elevation model to map climate across the U.S. from 1895−present, including regions impacted by high mountains, rain shadows, temperature inversions, coastal regions, and associated complex meso-scale climate processes. Using ArcGIS (ESRI, 2016), the data were clipped to the project boundary and used to calculate the average for our seven metrics (monthly temperature, precipitation, PET, surplus water, snow water equivalent, FMI, climate index, and seasonality of water surplus) for the normal period. Each of these metrics are inputs to or products of the HL classification process.

2.3.2 Historical climate analyses (1901−2010)

Unlike with monthly precipitation and temperature data, a time series of gridded daily historical climate data at a spatial resolution of 400 m was not available. Daily PRISM data is freely available at 4 km resolution, and this was what we used to develop the historical climate analyses for the 1901−2010 period. Gridded data for daily mean temperature and precipitation were clipped to the project boundary and averaged for each month over each decade (i.e., 1901−1910, 1911−1920, etc.). The data were then statistically downscaled to 400 m using the delta method (Hijmans et al., 2005; Ramirez-Villegas and Jarvis, 2010) to match the spatial resolution of the modern climate normal data (using the 400 m resolution, monthly PRISM climate normal for 1971−2000 period as the high resolution dataset). We acknowledge the inaccuracies and uncertainty imposed in the temperature and precipitation datasets by applying the downscaling functions to the original climate projections, however since these 400 m resolution monthly averages are normally distributed (Trzaska and Schnarr, 2014) and the data are to be aggregated to our 80 km^2 (on average) AUs, the trade-offs were deemed acceptable and preferable for characterizing the hydrology and climate for these analyses.

Using the approaches described herein, the downscaled data were used to calculate the average monthly PET, surplus water, snow water equivalent, FMI, and seasonality of water surplus for each decade. Summary figures were generated from this data depicting spatial distribution of climate and seasonality for each decade across the project area. These data were compared to the modern climate normals using spatially continuous time series analyses.

2.3.3 Future climate analyses (2041−2070)

In order to explore the potential range of modeled climatic response for the study area, we selected ten climate model projections from the full ensemble of World Climate Research Programme's Coupled Model Intercomparison Project phase 5 multi-model ensemble climate dataset projections (WCRP CMIP5; http://cmip-pcmdi.llnl.gov/cmip5; Taylor et al., 2012). These models are based on the Representative Concentration Pathway (RCP) 8.5 emissions scenario, which assumes the highest rate of emissions into the 21st century. We only used this emissions scenario to reduce the complexity of the analyses. To select the specific model simulations to use in this study, we created a scatterplot comparing future temperature and precipitation change for the different CMIP5 models over the project area. We selected ten models that spanned the range of predicted climatic responses of the full ensemble (Fig. 2), including drier, wetter, colder, and warmer responses. Average monthly precipitation and temperature for the ten projections (Table 1) were acquired from the monthly Bias-Correction and Spatial Disaggregation (BCSD) archive (Bureau of Reclamation, 2014) for the 2041−2070 period. These data were clipped to the project boundary and resampled to a 400 m grid using a bilinear approach (ESRI ArcGIS v10.4) to match the resolution and spatial extent of the modern climate normal data. The average monthly PET, surplus water, snow water equivalent, FMI, and seasonality of water surplus were calculated from the future climate data for each assessment unit. Summary figures were generated that illustrate the spatial distribution of climate and seasonality for each climate projection. The differences in FMI and seasonality of water surplus from the normal period were also mapped and compared.

2.4 Mapping vulnerability indices

As discussed in the introduction (Section 1), vulnerability can be measured by assessing the exposure, sensitivity, and adaptive capacity of a system to change (Adger, 2006; Füssel, 2007; Füssel and Klein, 2006; IPCC, 2014). Historic hydrology and climate are primary drivers for ecosystem change (Nelson, 2005), and are critical to certain industries and stakeholders in particular areas; thus historic hydrology and climate serve as proxies for the sensitivity of those systems to environmental change. In the assessment of hydrologic vulnerability, we evaluated the variability in historical climate data and our derived hydrologic metrics as a proxy for sensitivity. Likewise, we used future climate

https://doi.org/10.5194/hess-2019-638
Preprint. Discussion started: 23 January 2020

Hydrology and Earth System Sciences
Discussions

projections as a proxy for exposure to environmental change. Projections that fell outside of historic observations should then be associated with increased levels of exposure. In terms of adaptive capacity, we assumed that the systems present in a location are adapted to the historic observed variability in conditions. We also assumed that the systems would become stressed by conditions far outside of those previously experienced. Further, we suggest that the larger the number of future climate projections that exceed or fall far below their historic range, the more vulnerable a system associated with a particular climate will be with respect to climate-induced changes. Our hydrologic landscape vulnerability analysis (HLVA) places modern and projected environmental changes in the context of available historic data. The HLVA assesses vulnerability to changes in temperature, precipitation, potential evapotranspiration, snow accumulation, climatic moisture, surplus water, and seasonality of the water surplus by identifying areas that are projected to experience deviations from historic conditions.

The ten future climate projections (for the 2041−2070 period) were compared to the decadal averaged data from 1901−2010 for each AU. We calculated the historical standard deviation of each metric for each AU within the project area. For each metric, we assume that any projection that is within two-standard deviations of the historical climate values does not contribute to an increase in vulnerability, whereas projections outside of that range increase the vulnerability. We then define vulnerability for a given index as the number of the ten projections that are outside of the historical two-standard deviation threshold. Thus, the HLVA index assesses the likelihood that a given metric will exceed a two-standard deviation threshold from the decadal mean under future climate scenarios. A vulnerability index of ten indicates that all ten climate projections were beyond two-standard deviations from the historical mean and so are expected to experience projected conditions that they are not adapted to. The least vulnerable areas will have an index of zero, which indicates that all future climate projections fell within the two-standard deviation threshold to which systems are adapted to. The use of standard deviations is not an appropriate threshold metric for seasonality, because it is a categorical variable. For the seasonality metric, any projected seasonality value that has not been observed decadally between 1900 and 2010 increases the seasonality vulnerability index. For example, consider an AU that had predominantly experienced Spring seasonality, with the occasional Fall seasonality and that 7 of 10 climate models project Fall seasonality and 3 of 10 models predict Winter seasonality for 2041−2070. Since Winter seasonality was not observed for any decade between 1900 and 2010, the three predictions for Winter seasonality each contribute to the vulnerability index for seasonality. Finally, we analyzed the dominant HL code by area of the most vulnerable AUs (those having a vulnerability index greater than seven on a scale of ten) for each metric in order to gain insight about the dominant HL characteristics that relate to hydrologic vulnerability.

2.5 Locational time series analyses

Forty-five locations (Fig. 1 and Table 2) were selected for potential applications of the HL approach, based in part to demonstrate the method's relevance to potential water resource stakeholders to identify areas where we thought results could be of use to land managers. The time series for the decadal averages for each of the seven HL metrics were analyzed for the AUs associated with each of these locations. Decadal averages were plotted at the decadal midpoint for each 10-year period from 1901 to 2010. In addition, the 1971−2000 normal average for each variable and ten climate projections (2041−2070) were plotted in a similar manner. The HLVA was then used to determine the mean vulnerability index and the dominant HL code for the AUs associated with each location.

3 Results

3.1 Hydrologic landscape summary

Table 3 shows the percent coverage of the HL categories for the six states. Thirty percent of the region is mountainous (elevation relief of AU > 300 m and < 10 % of AU area has slope < 1 %) and 7 % is flat (AUs with more than 50 % area having < 1 % slope). The remaining area is classified as transitional. According to the soil permeability dataset (Miller and White, 1998) produced from the STATSGO soils database (Soil Survey Staff, 2016), 98 % of the surface soils (defined as the top 10 cm) are highly permeable (> 4.23 $\mu m\ s^{-1}$). Stratton et al. (2016) and Comeleo et al. (2014) classified the subsurface permeability of the six-state region as 60 % high permeability and 40 % low permeability. In terms of the 1971−2000 climate normal period, most of the area has the highest monthly water availability (seasonality) during the winter (63 %), fall (24 %), spring (13 %), with approximately 1 % experiencing summer seasonality. In addition, 30 % of the area is classified as having a moist, wet, or very wet climate, while 70 % is dry, semi-arid or arid. The HL maps for the study area (Washington, Oregon, Idaho, California, Nevada, and Arizona) are included in the appendix (Fig. A1). HL maps for the remainder of the conterminous US are also available and are also included as supplemental material (Fig. S1). Note that the subsurface permeability maps were not extended across the lower 48 states prior to submission but are available as supplemental material.

3.2 Climate analyses

3.2.1 Regional (spatially continuous) time series analyses

Figure 3 contains spatial trends in the change in FMI for the western U.S., showing wetter or drier decades relative to the 1971−2000 baseline period (Figure S2 in the supplemental material illustrates similar data for the continental US). Figure 4 displays projections of future (2041−2070) FMI values for the western U.S. relative to the 1971-2000 normal period, based on the ten climate projections (Figure S3 in the supplemental material illustrates similar data for the continental US). Three of the climate models (CCSM-R4, MRI-CGCM3, and CESM1) indicate that portions of the western U.S. may be wetter (as indicated by the blue areas in Fig. 4), while other areas will be drier (red) than or similar to the 1971−2000 normal. Similarly, the maps suggest that seven of the climate models (CCSM4, GFDL, inmcm4, CanESM2, HadGEM, CSIRO, and MIROC) project that much of the western U.S. will be considerably drier than the normal period. The remaining models indicate that some areas will be slightly drier, whereas much of the area will be similar to the 1971−2000 normal condition.

Figure 5 illustrates where the seasonal classes of surplus water have varied between 1901 and 2010 relative to the 1971−2000 base period (Figure S4 in the supplemental material illustrates similar data for the continental US). Most areas throughout this historical period show little variation in the season of maximum available water (i.e., are shown in white), but there are patterns in the water surplus seasonality that can be observed in the West. The 1940s, 1960s, 1980s, and 2000s seem to show later seasonality in southern Oregon and Idaho and Northern California and Nevada. In contrast, portions of Oregon, Washington, and Arizona are shown to have earlier seasonality in the 1900s, 1910s, 1930s, 1950s, and 1970s.

Figure 6 illustrates the seasonal changes in surplus water as projected by the ten climate models for 2041−2070 compared to 1971−2000 (Figure S5 in the supplemental material illustrates similar data for the continental US). In general, most of the climate models predict earlier surplus water in many of mountainous areas in the six western

https://doi.org/10.5194/hess-2019-638
Preprint. Discussion started: 23 January 2020

Hydrology and Earth System Sciences
Open Access
Discussions

states. Although most mountainous areas in Nevada are projected to have little change in seasonality, those that are projected to change are projected to have earlier seasonality. In Arizona, the White Mountains are predicted to have a later seasonality in two of ten climate projections (MIROC and GFDL), whereas seven projections predict earlier seasonality in western Arizona.

3.2.2 Vulnerability analyses

The vulnerability maps (Fig. 7) identify areas that are more or less subject to extreme future climatic and hydrologic variability (Similar vulnerability maps for the continental US are included in the supplemental materials (Fig. S6)). All climate projections indicate that temperature will change almost ubiquitously across the Pacific west, however changes in precipitation are much more spatially variable. The cold deserts and Mediterranean California Ecoregions (Level 2) are more consistently projected to experience changes in precipitation than has been observed since 1901 on a decadal basis. In contrast, major portions of Arizona, Washington, Oregon, and California have areas with low vulnerability to change with respect to precipitation. The Hamon (1961) method of calculating monthly PET uses temperature as the major input, so it is not surprising that the PET vulnerability map is similar to the temperature vulnerability map. The April 1 snow accumulation (snow water equivalent) vulnerability map seems to indicate that snow accumulation will change in many mountainous areas throughout the west, but particularly in the transitional areas when compared to the most snow prone areas of the West. S' is a measure of available water (excess water available for soil infiltration or overland flow). The map for S' suggests that the Warm Desert and Marine West Coast Forest Ecoregions are more likely to experience substantial changes in available water (i.e., high vulnerability) in the future. The FMI is calculated from the ratio of PET and precipitation per Eq. (1). The FMI vulnerability map indicates that the Cold Desert Ecoregions of central, Western Washington, the Warm Deserts of Southern California, and High Elevation Sierra Madre Mountains of south eastern Arizona are more likely to see substantial changes to the FMI. The regional time series analyses (below) provide more information about whether those areas are expected to become wetter or drier. The seasonality vulnerability map identifies AUs that are likely to have changes in seasonality. Portions of the Sierra-Nevada Mountains in California and the Cascades in Oregon, and mountainous areas in Idaho are projected to be more vulnerable to changes in seasonality. All other areas are not projected to be vulnerable to changes for seasonality.

3.2.3 Study area as a hydrologic landscape

Table 4 summarizes an analysis of the HL classifications of the most vulnerable AUs for each metric. For example, 75 % of the AUs identified as vulnerable for snow accumulation were classified as dry, moist, or wet, therefore very wet, semi-arid, and arid AUs are less likely to be vulnerable to changes in snow accumulation. Likewise, 76 % of AUs vulnerable to changes in seasonality had a spring seasonality during the 1971−2000 normal period. The physical properties represented by the dominant HL classes in Table 4 could help determine how various climate vulnerabilities are ultimately expressed. For example, vulnerability to changes in snow or FMI mostly occur in regions with wetter climates (Moist, Wet, or Very Wet climate), with fall or spring Seasonality, in areas with low subsurface permeability. This could result in increased precipitation, with quicker runoff in areas that currently have delayed release of water. Similarly, areas vulnerable to changes in surface runoff are arid landscapes with winter seasonality and highly

https://doi.org/10.5194/hess-2019-638
Preprint. Discussion started: 23 January 2020

Hydrology and Earth System Sciences
Discussions

permeable subsurface parent materials. This means that these changes in runoff could have a large impact on subsurface recharge and, ultimately, baseflow.

3.2.4 Locational time series

Historic and future changes in ecologically relevant variables are shown for three example locations (Napa-Sonoma Valley, Willamette Valley, Mt. Hood; Fig. 8). Similar analyses have been performed for areas of ecological, economic, or social significance (Table 2; see Appendix A (Fig. A2)). The number in the lower left corner of each graph in Fig. 8 indicates the vulnerability index for the specific metric and location. The vulnerability index for each location is also listed in Table 2 for each metric. For instance, precipitation at Mt. Hood has a vulnerability index of '3', which indicates that three of the climate projections exceed the threshold of two-standard deviations from the historic mean. Table 2 indicates that 81 % of the 834 km^2 area analyzed for Mt. Hood (Site #7) had an HL code of VsHMH, (very wet climate with spring seasonality, high subsurface permeability, mountainous terrain, and high surface permeability). During the normal period, sixty-one percent of the 1867 km^2 Napa-Sonoma Valley (Site #26) had an MwHMH HL classification, thus much of the area was classified as having a moist climate with winter seasonality, high subsurface permeability, mountain terrain, and high surface permeability. Eighty-three percent of the 1234 km^2 Willamette Valley AUs (Site #8) had an HL code of WfHTH during the normal period. Overall, the Willamette Valley had a wet climate, dominated by fall seasonality, high subsurface permeability, transitional terrain, and high surface permeability.

The time series in Fig. 8 (and Fig. A2) illustrate the trend in average decadal temperature, precipitation, SWE, PET, S', climate, and seasonality of water surplus. Note that each future (2041−2070) climate projection represents a single data point that represents the 2041 – 2070 30-year range and is connected to the 2001−2010 decade with a dotted red line. Additional figures for 41 other locations are provided in Appendix A (Fig. A2). Each of the three example areas is predicted to be warmer in the 2041−2070 future climate projections. Further, these projected temperatures are almost always outside of the historic (1901−2010) temperature range, and so all locations have high vulnerability with respect to future temperatures. None of the three examples show a strong trend relating to future precipitation projections. Mt. Hood appears to show increasing precipitation since 1901, but there is no evidence that the projected increases in precipitation are outside of historic behavior. Napa-Sonoma and the Willamette Valley have low vulnerability for change in snow, while Mt. Hood has high vulnerability for less April 1 snow accumulation in the 2041−2070 period. PET is calculated directly from temperature and therefore shows trends strongly correlated to temperature. There are no obvious trends in S' for the future projections for the selected examples; vulnerability of these sites for S' is low to moderate. The FMI projections for Napa-Sonoma Valley, the Willamette Valley and Mt. Hood are outside of two-standard deviations of historical trends in three to four out of ten of the projections (Table 2). In terms of seasonality, the vulnerability index is equal to zero in the Willamette and Napa-Sonoma Valleys. For Mt. Hood, vulnerability is low, with all of the future climate projections indicating that there will no longer be spring seasonality (the predominant historical season for runoff), but only 3 projections suggest that seasonality would transition to a winter seasonality that is not modeled to have occurred since at least 1900 on a decadal scale.

Hydrology and Earth System Sciences
Open Access
Discussions

4 Discussion

Vulnerability maps (Fig. 7) were developed that indicate what areas across the landscape are projected to experience conditions that exceed two-standard deviations of the historic decadal average conditions. These maps provide spatially explicit details about the areas of the landscape that are most likely to experience conditions outside of those observed previously for seven different climate indicators. These maps were developed to facilitate long-term planning for stakeholders to be able to assess their risk to climatic impacts. It is possible that ecosystems, businesses, and communities in areas mapped as vulnerable may not be able to adapt to the stresses imposed by future environmental conditions.

From the vulnerability maps (Fig. 7), it is apparent that temperature [similar to Nijssen et al. (2001)] and PET are consistently projected to exceed the two-standard deviation threshold of historic conditions for most regions, though changes in PET may be overestimated (Johnson et al., 2012; U.S. Environmental Protection Agency, 2013). Precipitation vulnerability maps are not as spatially uniform as temperature. The vulnerability maps for snow accumulation and S' (surplus water available for runoff or infiltration) show that the areas mapped as most vulnerable for the two metrics are almost reversed, other than central Idaho and the coastal areas of California, Oregon, and Washington. According to the snow vulnerability map, it appears that most areas that receive much snow are projected to experience significant changes in future snow accumulation. In a related study on snow cover, Nolin and Daly (2006) found that the areas with the warmest winter temperatures are most at risk of having no snow cover in the future. Regarding the Feddema Moisture Index, Fig. 7 suggests that most of the models indicate that the magnitude of the FMI change is mostly within two-standard deviations of normal. The seasonality vulnerability map (Fig. 7) shows that the high Sierra-Nevada mountains in California, the Cascade mountains, and the mountainous areas in Idaho are somewhat prone to changes in seasonality.

We used a retrospective analysis of PRISM climatic time series data to gain an understanding of the distribution of environmental conditions present since 1901. While others have mapped resource and hydrologic vulnerability (Hill et al., 2014; Nolin and Daly, 2006; Vorosmarty et al., 2000; Winter, 2000), we are aware of few that have used retrospective analyses to inform the mapping efforts (Deviney et al., 2006; Kim et al., 2011; O'Brien et al., 2004) and are not aware of studies that have mapped resource vulnerability at a large scale using these types of data. It is important to emphasize that our definition of vulnerability is based on agreement of models with respect to climate conditions that are outside of historic ranges. The inference is that systems dependent on historic climate conditions may not be adapted to future conditions, and so are vulnerable. It is possible that they have the adaptive capacity to maintain their ecological and economic systems, but this is not a certainty. The vulnerability maps do not show, however, watersheds or communities downstream of these source areas that would be impacted by these changes.

For this analysis, the 30-year normal climate conditions are compared to decadal (10-year) climate conditions since 1901. In addition, the 30-year normal for future projections (2041-2070) is compared to the historic range of decadal climate data. While this may appear to be a discrepancy in the analysis, it was included intentionally to represent a conservative approach to quantifying vulnerability indices. Normal conditions are averaged over a 30-year period and therefore exhibit less variability than decadal averages or annual averages. By examining the past variability of the decadal averages since 1901, we use a period that exhibits variability without being an entirely smooth dataset. We then compare that to the 30-year future climate normal, which inherently has much less variability. By using this approach, we recognize that we are not treating past data in the same manner as we treat future climate projections. We suggest that the resulting vulnerability conclusions are conservative, because if we had used decadal projections for future climate data, the range of output would have been more variable. Decadal data would potentially have increased our vulnerability indices for all parameters except those that are already at the maximum but should not have decreased the index in any case.

In Fig. 8, examples are provided (Napa-Sonoma Valley, Willamette Valley, and Mt. Hood) to illustrate how analyses, like the HLVA approach, can assist natural resource managers, business owners, or other stakeholders to understand the potential impacts that changes in climate may have on their environment and the local bottom line. It is necessary for a stakeholder to have an idea of the parameters most important to their ecosystem, industry, or resource of interest, and it should prove useful for land and resource managers that are seeking location specific information about potential climatic impacts (Glick et al., 2011; Lawler et al., 2010).

Important stakeholders in the western U.S. that may be expected to experience impacts from hydrological changes associated with climate include the wine and skiing industries. The Napa-Sonoma and Willamette Valleys are economically important for their grape vineyards and associated wineries. The Willamette Valley is recognized for the quality of its pinot noir varietals (http://wine.appellationamerica.com/wine-region/Willamette-Valley.html), which require narrower temperature ranges than other grape cultivars (Burakowski and Magnusson, 2012; Jones et al., 2010). Due to the importance of the pinot noir varietal to viticulturists in the Willamette Valley, they are likely more concerned with changes in temperature than FMI. The Napa-Sonoma region is recognized for a wider variety of grape cultivars (http://wine.appellationamerica.com/wine-region/Napa-Valley.html, Elliott-Fisk, 1993) that have higher tolerance for temperature fluctuations than the pinot noir varietals commonly grown in the Willamette Valley (Jones et al., 2010). Figure 8 indicates that both the Willamette Valley and Napa-Sonoma have temperature vulnerability indices of ten out of ten, and both have FMI vulnerability indices of three out of ten. These index values suggest that both locations are projected to have future temperatures that are significantly different than the historic observed temperatures. However, the Willamette Valley pinot noir vineyards may have more cause for concern, since pinot noir grapes are documented to be more sensitive to temperature. In the Napa and Sonoma Valleys, there may be less need for concern with temperature than in the Willamette Valley. In addition, while both locations have the same FMI vulnerability indices, Fig. 8 illustrates that FMI projections for Napa-Sonoma are much more variable than for the Willamette Valley. Thus, there is more uncertainty in the modeled water availability for Napa-Sonoma. Taken at face value, these modeled results suggest that a vintner growing warm temperature grape species in the Willamette Valley may have more confidence in his investments relative to a vintner in Napa-Sonoma, where there is more uncertainty regarding long-term water availability.

The skiing industry is also an important economic contributor. According to Burakowski and Magnusson (2012), the difference in economic impact between a high and low snowfall year for the State of Oregon is \$38.1 million, while California is estimated to lose more than \$75 million in low snow years. Mt. Hood is well known for its recreational snow sports and winter tourism in Oregon and would be impacted differently by the seven metrics than the Willamette and Napa-Sonoma examples (Fig. 8). Thus, resource managers and business leaders at Mt. Hood are likely more concerned about snow accumulation in their watershed than those in the wine and grape industries (although grape grower's ability to irrigate may be impacted by snow accumulation in the region). According to our analyses, Mt. Hood has a snow vulnerability index of seven out of a maximum of ten. The analysis of seasonality suggests some chance of a shorter ski season due to the spring runoff occurring earlier during the winter season. Even though these conditions have occurred in the past (Fig. 8), this may be much more deleterious to the economics of the modern or future ski industry than it was in the 1900s, because it contributed much less to the historic economy.

The quantity (as indicated by the FMI) and timing (as indicated by the seasonality of the water surplus) of moisture availability only account for a portion of the water balance for an area. The FMI and seasonality are assumed to be proxies for the quantity and timing of moisture availability, but when moisture is available as surface runoff, it may then infiltrate into the ground or act as surface runoff. Water may infiltrate the surface layer of soil (depending on the soil permeability) and may enter the subsurface layers (depending on the vertical conductivity of the subsurface layers). The velocity of water through the subsurface layers that flows towards a stream channel depend upon the horizontal conductivity of the subsurface layers. Thus, if the water was retained as surface or subsurface runoff, it may be transported more quickly in the downhill direction and into a stream channel depending upon the steepness of the terrain (included in the HL classification). As it relates to streamflow, the unique combination of the five HL characteristics (climate, seasonality, surface permeability, subsurface permeability, and terrain) allows for the estimation of catchment hydrologic responses to changes in temperature and climate (Leibowitz et al., 2014; Patil et al., 2014). The HL approach has proved useful for streamflow prediction in gaged basins for some HL classes and should be useful in many ungaged basins as well. However, this paper illustrates how the HL approach can help to assess climatic and hydrologic vulnerability across large spatial scales. The three examples we provided, show how the HLVA method could be useful to resource managers for considering how future climate conditions may impact important economic and conservation resources (for additional examples refer to the appendix (2).

5 Summary and conclusions

The hydrologic landscapes (HL) concept has proved useful for gaining a better understanding of hydrologic behaviour at the assessment unit and watershed scales across large geographic regions. By applying the HL concept to climatic and vulnerability analyses, we provide a planning approach that allows resource managers to consider historic and projected climate behavior in their long-term planning efforts so they can better assess the risk imposed by potential changes. The methodology also allows stakeholders to focus on particular areas of interest, which provides the flexibility necessary for the information to be relevant across applications and sectors. By applying the modified Wigington et al. (2013) HL approach across the western US, resource managers will gain a better understanding of the projected vulnerability of water resource availability in a large portion of the United States.

6 Data availability

The geospatial data files (Jones et al., 2020) will be uploaded to the GeoPlatform (https://www.geoplatform.gov) and EPA Environmental Dataset Gateway (https://edg.epa.gov). Data cannot be made publicly available and the DOI link cannot go activated until the paper is published per internal US EPA policy.

7 Code availability

Authors may deposit code in a FAIR-aligned repository/archive upon final acceptance of the manuscript for publication.

8 Video abstract

No video abstract is available at this time.

9 Author contribution

CJ and SL conceptualized the study with significant input from KS. CJ performed the formal analyses, investigation, developed the methodologies (with input from SL, KS, and RC), managed the project, developed the model code, performed the analyses, developed the final figures and tables, and wrote draft versions of the manuscript, and incorporated co-author feedback into the final version of the manuscript. SL supervised the project and performed project administration. RC contributed technical expertise regarding spatial data analyses and familiarity with hydrologic landscapes data analyses. RC and LS developed the subsurface permeability datasets. PM and CW provided and advice regarding the use of the future climate projections and the processing of those datasets.

10 Acknowledgements

We would like to thank James Markwiese, Mohammad Safeeq, and Eric Sproles for their constructive feedback on the manuscript. We also appreciate Jim Wigington’s insight and input on early drafts of our mapping products. We acknowledge the World Climate Research Programme's Working Group on Coupled Modelling, which is responsible for CMIP, and we thank the climate modeling groups (listed in Table 1 of this paper) for producing and making available their model output. For CMIP the U.S. Department of Energy's Program for Climate Model Diagnosis and Intercomparison provides coordinating support and led development of software infrastructure in partnership with the Global Organization for Earth System Science Portals. The information in this document has been funded entirely by the U.S. Environmental Protection Agency, in part through an appointment to the Internship/Research Participation Program at the Office of Research and Development, U.S. Environmental Protection Agency, administered by the Oak Ridge Institute for Science and Education through an interagency agreement between the U.S. Department of Energy and EPA, and also through Student Services Contract #EP-15-W-000041. The views expressed in this paper are those of the authors and do not necessarily reflect the views or policies of the U.S. Environmental Protection Agency. Any use of trade, firm, or product names is for descriptive purposes only and does not imply endorsement by the U.S. Government.

11 References

Adger, W. N.: Vulnerability, Glob. Environ. Chang., 16(3), 268–281, doi:10.1016/j.gloenvcha.2006.02.006, 2006.

https://doi.org/10.5194/hess-2019-638
Preprint. Discussion started: 23 January 2020

Hydrology and Earth System Sciences
Discussions

Barnett, T. P., Adam, J. C. and Lettenmaier, D. P.: Potential impacts of a warming climate on water availability in snow-dominated regions, Nature, 438(7066), 303–309, doi:10.1038/nature04141, 2005.

Battin, J., Wiley, M. W., Ruckelshaus, M. H., Palmer, R. N., Korb, E., Bartz, K. K. and Imaki, H.: Projected impacts of climate change on salmon habitat restoration, Proc. Natl. Acad. Sci. U. S. A., 104(16), 6720–6725, doi:10.1073/pnas.0701685104, 2007.

Brekke, L. D., Kiang, J. E., Olsen, J. R., Pulwarty, R. S., Raff, D. A., Turnipseed, D. P., Webb, R. S. and White, K. D.: Climate change and water resources management - A federal perspective: U.S. Geological Survey Circular 1331., 2009.

Brown, R. D. and Mote, P. W.: The response of Northern Hemisphere snow cover to a changing climate, J. Clim., 22(8), 2124–2145, doi:10.1175/2008JCLI2665.1, 2009.

Burakowski, E. and Magnusson, M.: Climate impacts on the winter tourism economy in the United States, Natl. Resour. Def. Counc., (December), 2012.

Bureau of Reclamation: Downscaled CMIP3 and CMIP5 Climate and Hydrology Projections: Release of Hydrology Projections, Comparison with preceding Information, and Summary of User Needs, Denver, Colrado, U.S.A., 2014.

Comeleo, R. L., Wigington Jr., P. J. and Leibowitz, S. G.: Creation of a digital aquifer permeability map for the Pacific Northwest (EPA/600/R-14/431), Corvallis, OR, USA., 2014.

Cook, B. I., Ault, T. R. and Smerdon, J. E.: Unprecedented 21st century drought risk in the American Southwest and Central Plains, Sci. Adv., 1(1), e1400082, doi:10.1126/sciadv.1400082, 2015.

Daly, C.: A new effort to update precipitation frequency maps for the United States., 2016a.

Daly, C.: PRISM Climate Group, Oregon State University, [online] Available from: http://prism.oregonstate.edu, 2016b.

Daly, C., Taylor, G. H., Gibson, W. P., Parzybok, T. W., Johnson, G. L. and Pasteris, P. A.: High-quality spatial climate data sets for the United States and beyond, Trans. ASAE, 43(6), 1957–1962, doi:10.13031/2013.3101, 2000.

Dettinger, M., Redmond, K. and Cayan, D.: Winter orographic precipitation ratios in the Sierra Nevada—Large-scale atmospheric circulations and hydrologic consequences, J. Hydrometeorol., 5(6), 1102–1116, doi:10.1175/JHM-390.1, 2004.

Dettinger, M. D.: Climate change, atmospheric rivers, and floods in California - A multimodel analysis of storm frequency and fagnitude changes, J. Am. Water Resour. Assoc., 47(3), 514–523, doi:10.1111/j.1752-1688.2011.00546.x, 2011.

Deviney, F. a., Rice, K. C. and Hornberger, G. M.: Time series and recurrence interval models to predict the vulnerability of streams to episodic acidification in Shenandoah National Park, Virginia, Water Resour. Res., 42(9), doi:10.1029/2005WR004740, 2006.

https://doi.org/10.5194/hess-2019-638
Preprint. Discussion started: 23 January 2020

Hydrology and Earth System Sciences
Open Access
Discussions

Elliott-Fisk, D. L.: Viticultural soils of California, with special reference to the Napa Valley, J. Wine Res., 4(2), 67–74, 1993.

ESRI: ArcGIS Desktop, [online] Available from: http://www.esri.com/, 2016.

Farley, K. A., Tague, C. and Grant, G. E.: Vulnerability of water supply from the Oregon Cascades to changing climate: Linking science to users and policy, Glob. Environ. Chang., 21(1), 110–122, doi:10.1016/j.gloenvcha.2010.09.011, 2011.

Feddema, J. J.: A revised Thornthwaite-type global climate classification, Phys. Geogr., 26(6), 442–466, doi:10.2747/0272-3646.26.6.442, 2005.

Füssel, H. M.: Vulnerability: A generally applicable conceptual framework for climate change research, Glob. Environ. Chang., 17(2), 155–167, doi:10.1016/j.gloenvcha.2006.05.002, 2007.

Füssel, H. M. and Klein, R. J. T.: Climate change vulnerability assessments: An evolution of conceptual thinking, Clim. Change, 75(3), 301–329, doi:10.1007/s10584-006-0329-3, 2006.

Glick, P., Stein, B. A. and Edelson, N. A., Eds.: Scanning the conservation horizon: A guide to climate change vulnerability assessment, National Wildlife Federation, Washington D.C., USA., 2011.

Hamlet, A. F.: Assessing water resources adaptive capacity to climate change impacts in the Pacific Northwest Region of North America, Hydrol. Earth Syst. Sci., 15(5), 1427–1443, doi:10.5194/hess-15-1427-2011, 2011.

Hamon, W. R.: Estimating potential evapotranspiration, J. Hydraul. Div., 87(3), 1961.

Hidalgo, H. G., Das, T., Dettinger, M. D., Cayan, D. R., Pierce, D. W., Barnett, T. P., Bala, G., Mirin, A., Wood, A. W., Bonfils, C., Santer, B. D. and Nozawa, T.: Detection and attribution of streamflow timing changes to climate change in the western United States, J. Clim., 22(13), 3838–3855, doi:10.1175/2009JCLI2470.1, 2009.

Hijmans, R. J., Cameron, S. E., Parra, J. L., Jones, P. G. and Jarvis, A.: Very high resolution interpolated climate surfaces for global land areas, Int. J. Climatol., 25(15), 1965–1978, doi:10.1002/joc.1276, 2005.

Hill, R. A., Hawkins, C. P. and Carlisle, D. M.: Predicting thermal reference conditions for USA streams and rivers, Freshw. Sci., 32(1), 39–55, doi:10.1899/12-009.1, 2013.

Hill, R. A., Hawkins, C. P. and Jin, J.: Predicting thermal vulnerability of stream and river ecosystems to climate change, Clim. Change, 125(3–4), 399–412, doi:10.1007/s10584-014-1174-4, 2014.

IPCC: Climate Change 2014: Impacts, Adaptation, and Vulnerability, edited by C. B. Field, V. R. Barros, D. J. Dokken, K. J. Mach, M. D. Mastrandrea, T. E. Bilir, M. Chatterjee, K. L. Ebi, Y. O. Estrada, R. C. Genova, B. Girma, E. S. Kissel, A. N. Levy, S. MacCracken, P. R. Mastrandrea, and L. L. White, Cambridge University Press, Cambridge, UK and New York, NY, USA., 2014.

Johnson, T. E., Butcher, J. B., Asce, M., Parker, A. and Weaver, C. P.: Investigating the Sensitivity of U.S. Streamflow and Water Quality to Climate Change: U.S. EPA Global Change Research Program' s 20 Watersheds Project, J. Water Resour. Plan. Mangement, 138(5), 453–464, doi:10.1061/(ASCE)WR.1943-5452.0000175., 2012.

https://doi.org/10.5194/hess-2019-638
Preprint. Discussion started: 23 January 2020

Jones Jr., C. E. , Leibowitz, S.G., Comeleo, R.L., and Stratton, L.E.: Hydrologic Landscape Vulnerability Assessment Data. EPA Environmental Dataset Gateway. doi:10.23719/1504217, 2020 (Data cannot be made publicly available and the DOI link cannot go activated until the paper is published per internal US EPA policy).

Jones, G. V., Duff, A. A., Hall, A. and Myers, J. W.: Spatial analysis of climate in winegrape growing regions in the western United States, Am. J. Enol. Vitic., 61, 313–326, 2010.

Jung, I. W. and Chang, H.: Climate change impacts on spatial patterns in drought risk in the Willamette River Basin, Oregon, USA, Theor. Appl. Climatol., 108(3–4), 355–371, doi:10.1007/s00704-011-0531-8, 2012.

Kim, D. H., Yoo, C. and Kim, T. W.: Application of spatial EOF and multivariate time series model for evaluating agricultural drought vulnerability in Korea, Adv. Water Resour., 34(3), 340–350, doi:10.1016/ j.advwatres.2010.12.010, 2011.

Lawler, J. J., Tear, T. H., Pyke, C., Shaw, R. M., Gonzalez, P., Kareiva, P., Hansen, L., Hannah, L., Klausmeyer, K., Aldous, A., Bienz, C. and Pearsall, S.: Resource management in a changing and uncertain climate, Front. Ecol. Environ., 8(1), 35–43, doi:10.1890/070146, 2010.

Leibowitz, S. G., Wigington Jr., P. J., Comeleo, R. L. and Ebersole, J. L.: A temperature-precipitation-based model of thirty-year mean snowpack accumulation and melt in Oregon, USA, Hydrol. Process., 26, 741–759, doi:10.1002/hyp.8176, 2012.

Leibowitz, S. G., Comeleo, R. L., Wigington Jr., P. J., Weaver, C. P., Morefield, P. E., Sproles, E. A. and Ebersole, J. L.: Hydrologic landscape classification evaluates streamflow vulnerability to climate change in Oregon, USA, Hydrol. Earth Syst. Sci., 18(9), 3367–3392, doi:10.5194/hess-18-3367-2014, 2014.

Leibowitz, S. G., Comeleo, R. L., Wigington Jr., P. J., Weber, M. H., Sproles, E. A. and Sawicz, K. A.: Hydrologic landscape characterization for the Pacific Northwest, USA, J. Am. Water Resour. Assoc., 52(2), n/a-n/a, doi:10.1111/1752-1688.12402, 2016.

Luce, C. H. and Holden, Z. A.: Declining annual streamflow distributions in the Pacific Northwest United States, 1948−2006, Geophys. Res. Lett., 36(16), 2–7, doi:10.1029/2009GL039407, 2009.

Mancosu, N., Snyder, R., Kyriakakis, G. and Spano, D.: Water Scarcity and Future Challenges for Food Production, Water, 7(3), 975–992, doi:10.3390/w7030975, 2015.

Mann, M. E. and Gleick, P. H.: Climate change and California drought in the 21st century:, Proc. Natl. Acad. Sci., 112(13), 39313936, doi:10.1073/pnas.1503667112, 2015.

Maurer, D. K., Lopes, T. J., Medina, R. L. and Smith, J. L.: Hydrogeology and hydrologic landscape regions of Nevada, Carson City, NV., 2004.

McAfee, S. A.: Methodological differences in projected potential evapotranspiration, Clim. Change, 120(4), 915–930, doi:10.1007/s10584-013-0864-7, 2013.

McKay, L., Bondelid, T., Dewald, T., Johnston, J., Moore, R. and Rea, A.: NHDPlus Version 2: User Guide., 2012.

https://doi.org/10.5194/hess-2019-638
Preprint. Discussion started: 23 January 2020

Hydrology and Earth System Sciences
Open Access
Discussions

Mekonnen, M. and Hoekstra, A.: Four Billion People Experience Water Scarcity, Sci. Adv., (2), 1–7, doi:10.1126/sciadv.1500323, 2016.

Melillo, J. M., Richmond, T. C. and Yohe, G. W., Eds.: Climate Change Impacts in the United States: The Third National Climate Assessment., 2014.

Miller, D. A. and White, R. A.: A conterminous United States multi-layer soil characteristics data set for regional climate and hydrology modeling, Earth Interact. 2 [online] Available from: http://earthinteractions.org, 1998.

Mock, C. J.: Climatic controls and spatial variations of precipitation in the western United States, J. Clim., 9(5), 1111–1124, doi:10.1175/1520-0442(1996)009<1111:CCASVO>2.0.CO;2, 1996.

Mote, P. W., Hamlet, A. F., Clark, M. P. and Lettenmaier, D. P.: Declining mountain snowpack in western North America, Bull. Am. Meteorol. Soc., 86(1), 39–49, doi:10.1175/BAMS-86-1-39, 2005.

National Intelligence Council: Global Water Security: Intelligence Community Assessment (ICA 2012-08), Washington D.C., USA. [online] Available from: https://www.dni.gov/files/documents/Special Report_ICA Global Water Security.pdf, 2012.

Nelson, G. C.: Chapter 3. Drivers of Ecosystem Change: Summary Chapter, Island Press, Washington D.C., USA., 2005.

Nijssen, B., O'Donnell, G. M., Hamlet, A. F. and Lettenmaier, D. P.: Hydrologic Sensitvity of Global Rivers to Climate Change, Clim. Change, 50(1), 143–175 [online] Available from: http://www.springerlink.com/index/M24116121218031X.pdf (Accessed 29 July 2011), 2001.

NOAA State Climate Extremes Committee: Climatic Extreme Records, NOAA Natl. Centers Environ. Inf. [online] Available from: http://www.ncdc.noaa.gov/extremes/scec/records (Accessed 18 November 2018), 2016.

Nolin, A. W.: Perspectives on climate change, mountain hydrology, and water resources in the Oregon Cascades, USA, Mt. Res. Dev., 32, S35–S46, doi:10.1659/MRD-JOURNAL-D-11-00038.S1, 2011.

Nolin, A. W. and Daly, C.: Mapping "at risk" snow in the Pacific Northwest, J. Hydrometeorol., 7, 1164–1171, doi:10.1175/JHM543.1, 2006.

O'Brien, K., Leichenko, R., Kelkar, U., Venema, H., Aandahl, G., Tompkins, H., Javed, A., Bhadwal, S., Barg, S., Nygaard, L. and West, J.: Mapping vulnerability to multiple stressors: Climate change and globalization in India, Glob. Environ. Chang., 14(4), 303–313, doi:10.1016/j.gloenvcha.2004.01.001, 2004.

Patil, S. D., Wigington Jr., P. J., Leibowitz, S. G. and Comeleo, R. L.: Use of hydrologic landscape classification to diagnose streamflow predictability in Oregon, J. Am. Water Resour. Assoc., 50(3), 762–776, doi:10.1111/jawr.12143, 2014.

Ramirez-Villegas, J. and Jarvis, A.: Downscaling global circulation model outputs: The delta method decision and policy analysis working paper No. 1, Cali, Columbia. [online] Available from: http://ccafs-climate.org/downloads/docs/Downscaling-WP-01.pdf, 2010.

Safeeq, M., Grant, G. E., Lewis, S. L., Kramer, M. G. and Staab, B.: A hydrogeologic framework for characterizing summer streamflow sensitivity to climate warming in the Pacific Northwest, USA, Hydrol. Earth Syst. Sci., 18(9), 3693–3710, doi:10.5194/hess-18-3693-2014, 2014.

Siler, N., Roe, G. and Durran, D.: On the dynamical causes of variability in the rain-shadow effect: A case study of the Washington Cascades, J. Hydrometeorol., 14(1), 122–139, doi:10.1175/JHM-D-12-045.1, 2013.

Soil Survey Staff: Web Soil Survey, Nat. Resour. Conserv. Serv. USDA [online] Available from: http://websoilsurvey.nrcs.usda.gov (Accessed 18 May 2016), 2016.

Stratton, L., Comeleo, R. L., Leibowitz, S. G. and Wigington Jr., P. J.: Development of a digital aquifer permeability map for the pacific southwest in support of the hydrologic landscape classification: Methods (EPA/600/R-16/063), Corvallis, OR, USA. [online] Available from: https://nepis.epa.gov/Exe/ZyPDF.cgi/P100PB7N.PDF?Dockey=P100PB7N.PDF, 2016.

Tague, C. and Grant, G. E.: A geological framework for interpreting the low-flow regimes of Cascade streams, Willamette River Basin, Oregon, Water Resour. Res., 40(4), 1–9, doi:10.1029/2003WR002629, 2004.

Tague, C. L., Choate, J. S. and Grant, G.: Parameterizing sub-surface drainage with geology to improve modeling streamflow responses to climate in data limited environments, Hydrol. Earth Syst. Sci., 17(1), 341–354, doi:10.5194/hess-17-341-2013, 2013.

Tansel, B.: Hydrologic vulnerability and preventing domino effect consequences, Hydrol. Curr. Res., 4(4), 10–11, doi:10.4172/2157-7587.1000e11, 2013.

Taylor, K. E., Stouffer, R. J. and Meehl, G. A.: An overview of CMIP5 and the experiment design, Bull. Am. Meteorol. Soc., 93(4), 485–498, doi:10.1175/BAMS-D-11-00094.1, 2012.

Thompson, D. W. and Wallace, J. M.: Regional climate impacts of the Northern Hemisphere annular mode, Science, 293, 85–89, doi:10.1126/science.1058958, 2001.

Todd, M. J., Wigington Jr., P. J. and Sproles, E. A.: Hydrologic landscape classification to estimate Bristol Bay, Alaska watershed hydrology, JAWRA J. Am. Water Resour. Assoc., 53(5), 1008–1031, doi:https://doi.org/10.1111/1752-1688.12544, 2017.

Trzaska, S. and Schnarr, E.: A Review of Downscaling Methods for Climate Change Projections, Burlington, VT, USA., 2014.

U.S. Environmental Protection Agency: Watershed modeling to assess the sensitivity of streamflow, nutrient and sediment loads to potential climate change and urban development in 20 U.S. Watersheds (EPA/600/R-12/058F), Washington D.C., USA., 2013.

U.S. Global Change Research Program: The United States National Climate Assessment. Uses of Vulnerablity Assessments for the National Climate Assessment. NCA Report Series, Volume 9., Washington D.C., USA. [online] Available from: http://www.globalchange.gov/browse/reports?f%5B0%5D=field_report_year:171, 2011.

https://doi.org/10.5194/hess-2019-638
Preprint. Discussion started: 23 January 2020

Vano, J. A., Nijssen, B. and Lettenmaier, D. P.: Seasonal hydrologic responses to climate change in the Pacific Northwest, Water Resour. Res., 6(4), 1–18, doi:10.1002/2014WR015909, 2015.

Vorosmarty, C. J., Green, P., Salisbury, J. and Lammers, R. B.: Global water resources: Vulnerability from climate change and population growth, Science, 289, 284–288, doi:10.1126/science.289.5477.284, 2000.

Watson, J. E. M., Iwamura, T. and Butt, N.: Mapping vulnerability and conservation adaptation strategies under climate change, Nat. Clim. Chang., 3(11), 989–994, doi:10.1038/nclimate2007, 2013.

Wigington Jr., P. J., Leibowitz, S. G., Comeleo, R. L. and Ebersole, J. L.: Oregon hydrologic landscapes: A classification framework, J. Am. Water Resour. Assoc., 49(1), 163–182, doi:10.1111/jawr.12009, 2013.

Winter, T. C.: The vulnerability of wetlands to climate change: a hydrologic landscape perspective, J. Am. Water Resour. Assoc., 36(2), 305–311, doi:10.1111/j.1752-1688.2000.tb04269.x, 2000.

Winter, T. C.: The concept of hydrologic landscapes, J. Am. Water Resour. Assoc., 37(2), 335–349, 2001.

Wolock, D. M., Winter, T. C. and McMahon, G.: Delineation and evaluation of hydrologic-landscape regions in the United States using geographic information system tools and multivariate statistical analyses, Environ. Manage., 34, S71–S88, doi:10.1007/s00267-003-5077-9, 2004.

https://doi.org/10.5194/hess-2019-638
Preprint. Discussion started: 23 January 2020

12 Figures

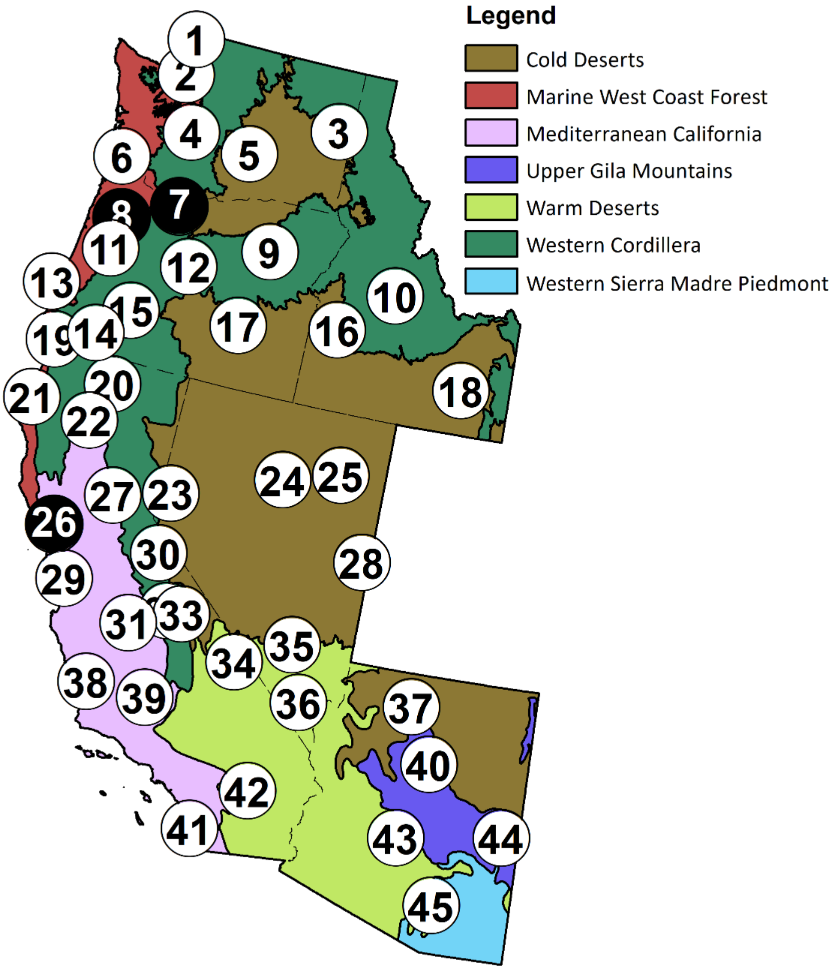

Figure 1. Study area showing map with the six states of WA, OR, ID, CA, NV, and AZ. Also shown are the 7 EPA Level II Ecoregions and 45 locations identified by numbered circles with three example locations in black circles (Table 2).

https://doi.org/10.5194/hess-2019-638
Preprint. Discussion started: 23 January 2020

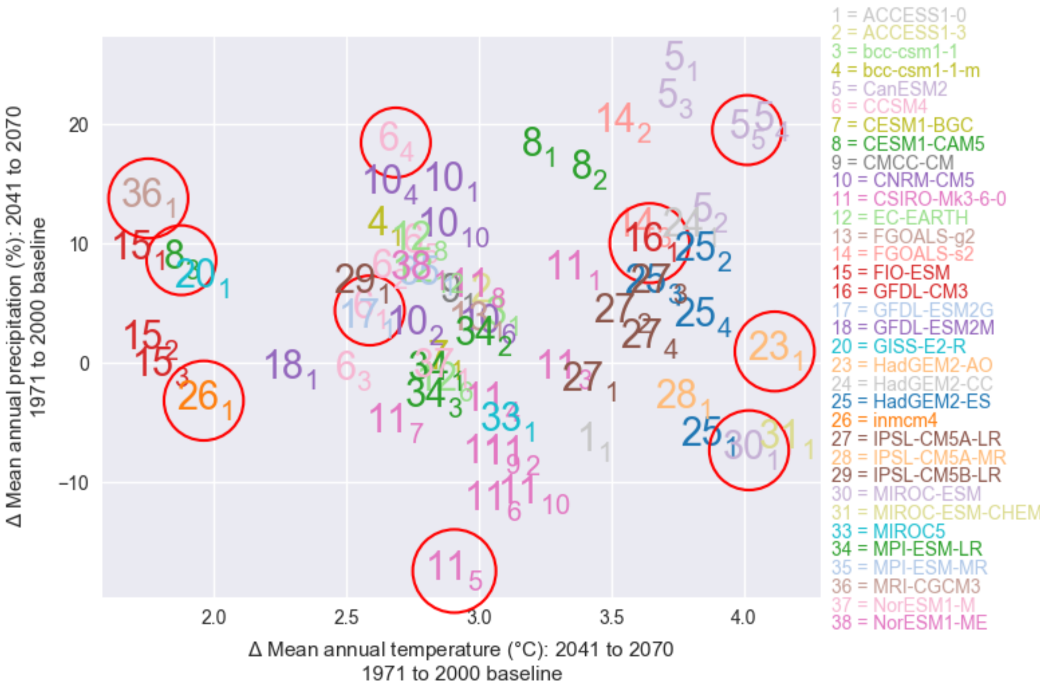

Figure 2. Scatterplot showing the range of mean temperature and precipitation projections for the 2041−2070 climate models across the study area. The circled data points identify the climate projections used in our analyses.

https://doi.org/10.5194/hess-2019-638
Preprint. Discussion started: 23 January 2020

Hydrology and Earth System Sciences
Discussions
Open Access

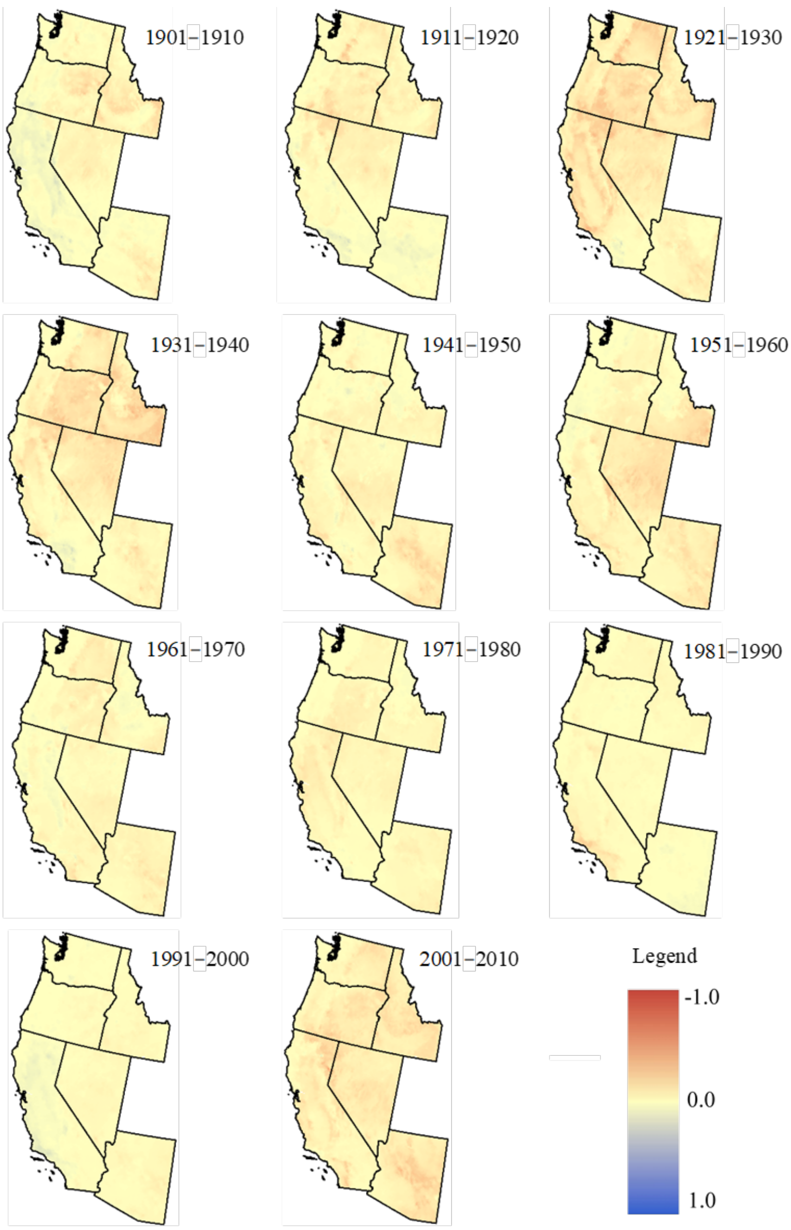

Figure 3. Decadal change in Feddema Moisture Index relative to 1971−2000 normal period. Red and blue colors indicate drier and wetter average conditions than 1971−2000, respectively.

https://doi.org/10.5194/hess-2019-638
Preprint. Discussion started: 23 January 2020

Hydrology and Earth System Sciences
Open Access
Discussions

756 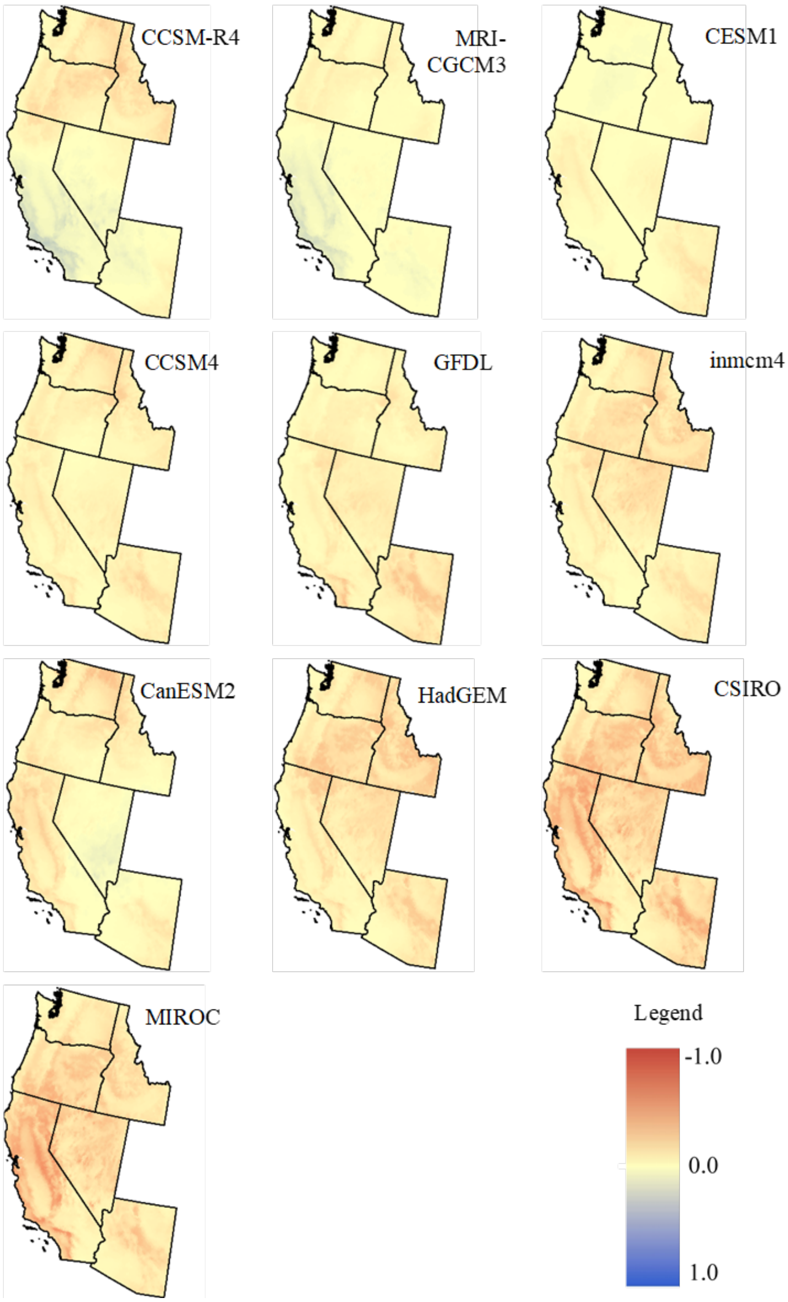

757 **Figure 4. Projected change in Feddema Moisture Index for 2041−2070 relative to 1971−2000 for ten climate models (Table**
758 **1). Red and blue colors indicate drier and wetter conditions than the 1971−2000 base period, respectively. Abbreviated**
759 **model names correlate to those in Table 1.**

https://doi.org/10.5194/hess-2019-638
Preprint. Discussion started: 23 January 2020

Hydrology and Earth System Sciences
Open Access
Discussions

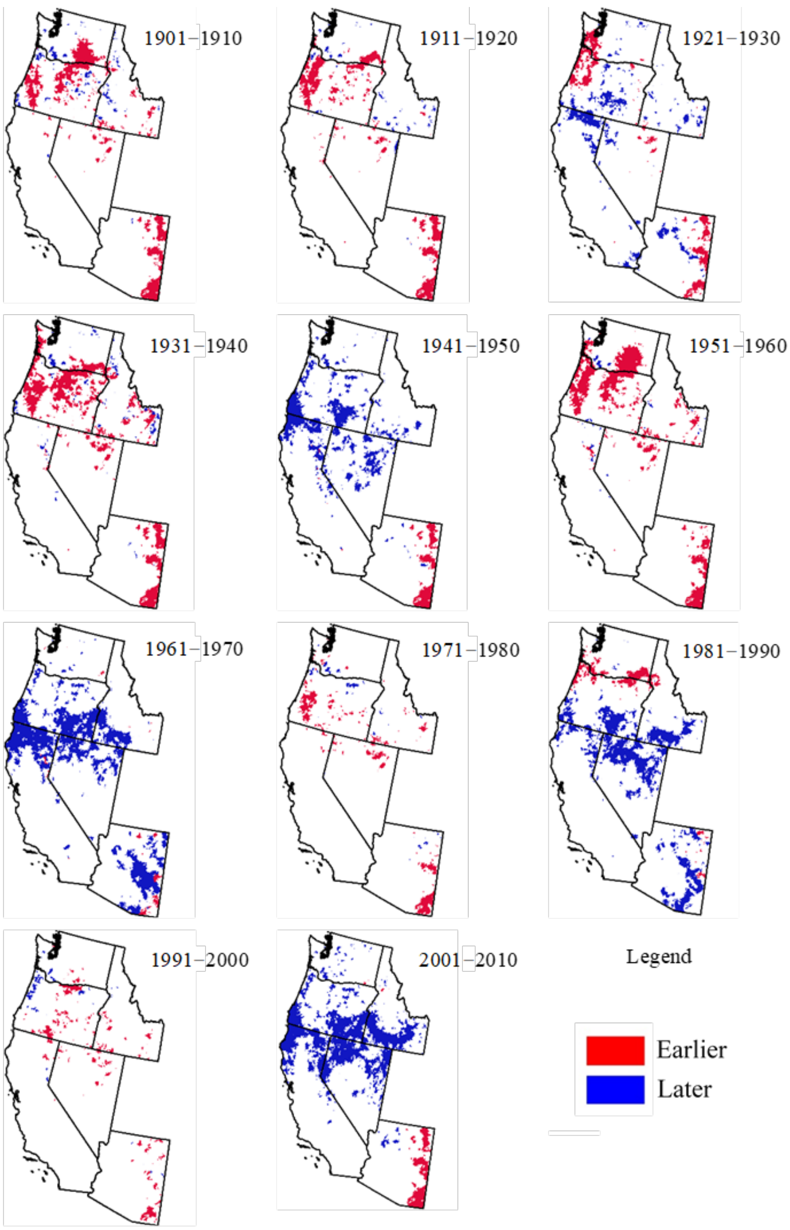

760

761 **Figure 5. Decadal change in seasonality of water surplus since 1901 relative to 1971−2000. Red and blue colors indicate**
762 **earlier and later seasonality than the 1971−2000 base period, respectively.**

https://doi.org/10.5194/hess-2019-638
Preprint. Discussion started: 23 January 2020

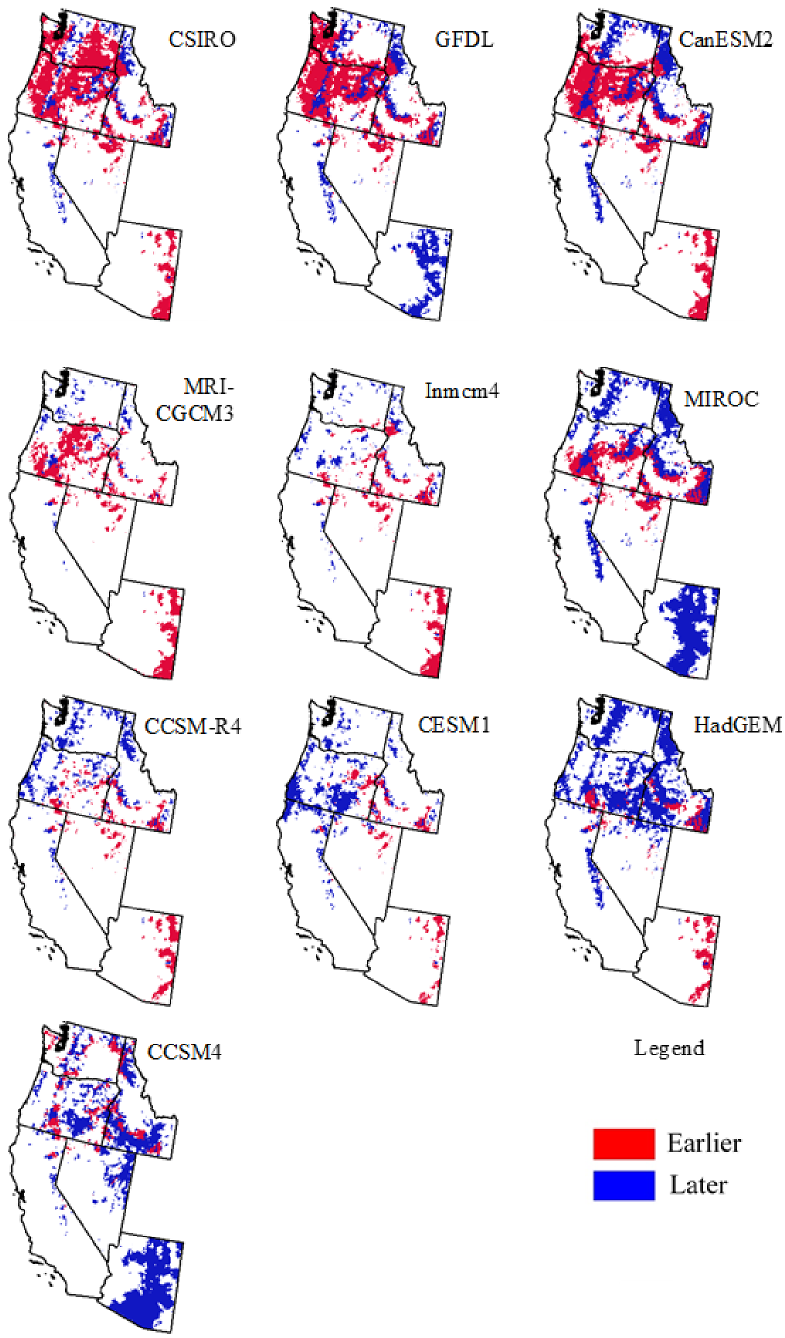

Figure 6. Projected change in seasonality of water surplus for 2041−2070 relative to 1971−2000 for ten climate models. Red and blue colors indicate earlier and later seasonality than the 1971−2000 base period, respectively. Abbreviated model names correlate to those in Table 1.

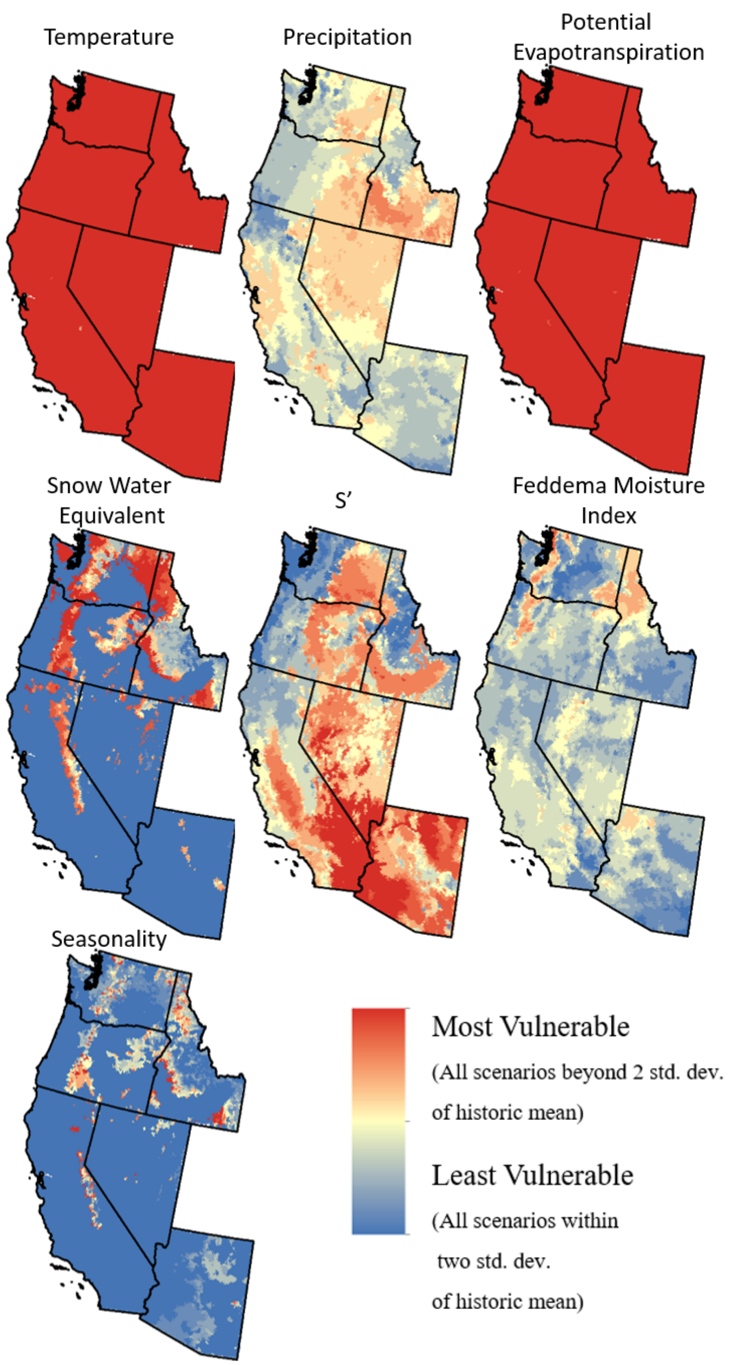

Figure 7. Vulnerability indices for temperature, precipitation, potential evapotranspiration, snow water equivalent (April 1), S' (available water), Feddema Moisture Index, and seasonality. The least vulnerable locations are those projected to be within two-standard deviations of the historic (1901−2010) mean in all nine climate models.

https://doi.org/10.5194/hess-2019-638
Preprint. Discussion started: 23 January 2020

Hydrology and Earth System Sciences
Open Access
Discussions

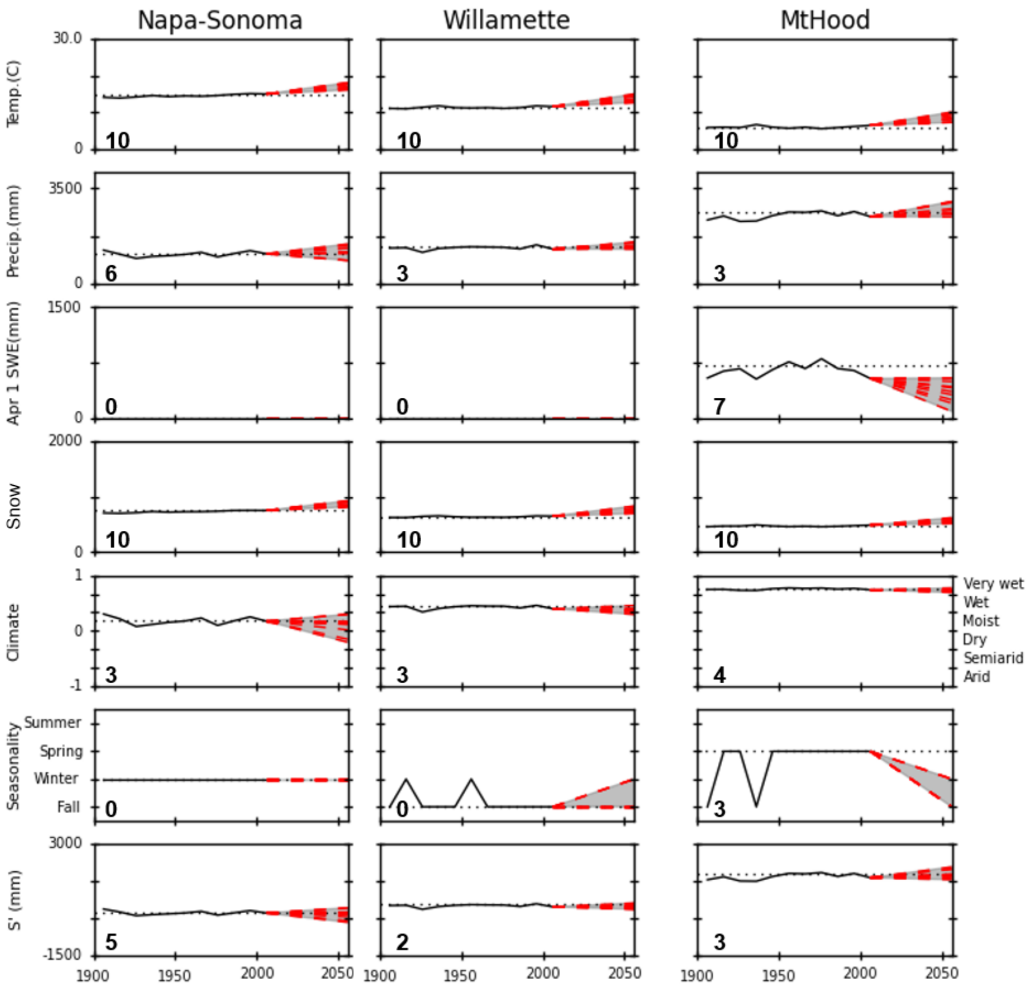

Figure 8. Time series of average decadal temperature, precipitation, snow (April 1 snow water equivalent (mm)), potential evapotranspiration (PET), available water (S'), FMI, and seasonality for three specific locations in the western U.S. Dotted black line represents the 1971−2000 base period; the dashed red line connects the 2001−2010 value to the 2041−2070 climate projections. The number in lower left indicates the vulnerability index for the metric and location depicted in the associated graph.

https://doi.org/10.5194/hess-2019-638
Preprint. Discussion started: 23 January 2020

Hydrology and Earth System Sciences
Open Access
EGU
Discussions

13 Tables

Table 1. CMIP5 Climate model summary for 2041−2070 precipitation and temperature data (Bureau of Reclamation, 2014).

WCRP CMIP5 Climate Model	Model abbreviated name	Model realization used herein	Abbreviated name used in this paper for realization
Canadian Earth System Model	CanESM2	r5i1p1	CanESM2
Community Climate System Model	CCSM4	r1i1p1	CCSM4
Community Climate System Model	CCSM4	r4i1p1	CCSM4-R4
Community Earth System Model	CESM1	r3i1p1	CESM1
Commonwealth Scientific and Industrial Research Organisation Mark 3.6	CSIRO-Mk3-6-0	r5i1p1	CSIRO
Geophysical Fluid Dynamics Laboratory Coupled Climate Model	GFDL-CM3	r1i1p1	GFDL
Hadley Global Environment Model	HadGEM2-AO	r1i1p1	HadGem
Institute for Numerical Mathematics Climate Model	INM-CM4	r1i1p1	inmcm4
Model for Interdisciplinary Research on Climate	MIROC-ESM	r1i1p1	MIROC
Meteorological Research Institute	MRI-CGCM3	r1i1p1	MRI-CGCM3

https://doi.org/10.5194/hess-2019-638
Preprint. Discussion started: 23 January 2020

Hydrology and Earth System Sciences
Open Access
EGU
Discussions

Table 2. Summary table for 45 study locations (sorted by decreasing latitude) provides numeric ID from Fig. 1, total analysis area, dominant HL class (representing climate, seasonality, subsurface permeability, terrain, and surface permeability), percent area represented by dominant HL class, latitude and longitude of the center point of the area, and vulnerability indices for temperature, potential evapotranspiration (PET), precipitation, S', snow, Feddema Moisture Index (FMI), and seasonality.

Site #	Name	Area (km^2)	Dominant HL Class*	% Dominant Area	Coordinates Lat.	Coordinates Long.	Vulnerability Index Temp.	PET	Precip.	S'	Snow	FMI	Seasonality
1	Bellingham	212	WfLTH	99 %	48.77	-122.45	10	10	5	1	0	9	0
2	Spokane	592	DfHTH	80 %	47.64	-117.43	10	10	6	7	10	3	1
3	Seattle	669	WfLTH	78 %	47.60	-122.25	10	10	4	1	0	5	2
4	MtRainier	718	VsLMH	76 %	46.85	-121.79	10	10	4	2	7	4	2
5	Yakima	438	SfHTH	86 %	46.63	-120.60	10	10	3	6	0	0	0
6	Portland	932	WfHTH	67 %	45.53	-122.66	10	10	3	2	0	6	0
7	MtHood	834	VsHMH	81 %	45.37	-121.70	10	10	3	3	7	4	3
8	UmatillaNF	2,147	MsLMH	29 %	44.87	-118.70	10	10	6	3	6	3	4
9	Willamette	1,234	WfHTH	83 %	44.84	-123.14	10	10	3	2	0	4	0
10	ChallisNF	4,348	WsLMH	74 %	44.55	-114.75	10	10	6	0	3	2	0
11	Bend	948	SfHTH	68 %	44.21	-121.26	10	10	4	8	0	3	0
12	Eugene	523	WfHFH	64 %	44.10	-123.15	10	10	3	1	0	2	0
13	Boise	594	SwHTH	51 %	43.61	-116.24	10	10	8	8	0	2	0
14	MalheurNWR	1,355	SwHFH	69 %	43.27	-119.04	10	10	6	7	0	2	0
15	CraterLake	1,721	WsHTH	45 %	42.98	-122.08	10	10	3	2	9	3	10
16	Pocatello	349	DwHTH	45 %	42.88	-112.43	10	10	7	7	0	1	0
17	SiskiyouNF	926	VwLMH	100 %	42.36	-124.29	10	10	2	0	0	2	0
18	Medford	375	DfLTH	60 %	42.34	-122.89	10	10	1	5	0	2	0
19	SixRivers	1,527	VwLMH	100 %	41.63	-123.79	10	10	2	2	0	4	0
20	MtShasta	956	WwHMH	49 %	41.36	-122.23	10	10	1	2	0	3	0
21	RubyMtn	1,132	DfLTH	44 %	40.68	-115.31	10	10	6	5	9	4	0
22	Arcata-HumboldtCo	2,511	WwLMH	63 %	40.62	-124.01	10	10	3	2	0	3	0
23	Redding	478	MwHTH	59 %	40.56	-122.38	10	10	2	2	0	2	0
24	BattleMtn	902	SwLMH	75 %	40.09	-116.71	10	10	6	7	0	4	0
25	Reno	382	SwHTH	40 %	39.54	-119.80	10	10	4	7	0	3	0

https://doi.org/10.5194/hess-2019-638
Preprint. Discussion started: 23 January 2020

Site #	Name	Area (km^2)	Dominant HL Class*	% Dominant Area	Coordinates		Vulnerability Index							
					Lat.	Long.	Temp.	PET	Precip.	S'	Snow	FMI	Seasonality
26	GreatBasinNP	38	MsLMH	100 %	39.01	-114.26	10	10	4	5	0	4	1
27	Sacramento	855	SwHFH	88 %	38.57	-121.39	10	10	6	7	0	3	0
28	Napa-Sonoma	1,867	MwHTH	61 %	38.37	-122.53	10	10	6	5	0	3	0
29	YosemiteNP	2,455	VsLMH	44 %	37.93	-119.55	10	10	4	4	9	3	0
30	SanFranciscoBay	3,356	DwHMH	19 %	37.44	-122.29	10	10	6	5	0	5	0
31	SierraNF	5,349	WwLMH	31 %	37.17	-119.05	10	10	4	4	0	2	0
32	HighSierras	2,239	WsLMH	32 %	37.15	-118.81	10	10	2	4	1	2	0
33	NevadaTestSite	3,121	AwHMH	67 %	36.96	-116.22	10	10	5	10	0	4	0
34	Fresno	1,393	AwHFH	100 %	36.74	-119.91	10	10	5	8	0	4	0
35	DeathValleyNP	7,862	AwHMH	50 %	36.45	-117.03	10	10	5	10	0	5	0
36	LasVegas	977	AwHTH	65 %	36.23	-115.26	10	10	4	10	0	4	0
37	GrandCanyonNP	3,475	SwHMH	28 %	36.22	-112.11	10	10	4	10	0	6	0
38	SanLuisObispo	2,653	DwLMH	98 %	35.36	-120.63	10	10	4	4	0	4	0
39	Bakersfield	3,399	AwHFH	96 %	35.33	-119.14	10	10	4	9	0	4	0
40	Flagstaff	365	DwHMH	51 %	35.19	-111.60	10	10	3	4	0	4	0
41	JoshuaTreeNP	2,599	AwLMH	68 %	33.92	-115.99	10	10	5	7	0	5	0
42	WhiteMtns	4,855	WfLMH	23 %	33.87	-109.53	10	10	4	3	0	3	0
43	Phoenix	2,304	AwHFH	63 %	33.52	-112.11	10	10	3	10	0	2	1
44	SanDiego	1,276	SwLMH	37 %	32.90	-117.06	10	10	4	6	0	4	0
45	Tucson	1,838	AwHTH	62 %	32.19	-110.95	10	10	3	9	0	1	2

*Climate class (1st letter): V=very wet; W=wet; M=moist; D=dry; S=semiarid; A=arid
Seasonality class (2nd letter): f=fall; w= winter; s=spring; u=summer
Subsurface permeability class (3rd letter): L=low; H=high
Terrain class (4th letter): M=mountain; T=transitional; F=flat
Surface permeability class (5th letter): L=low; H=high

https://doi.org/10.5194/hess-2019-638
Preprint. Discussion started: 23 January 2020

Table 3. Percent of area of each HL category and classification within the six-state region (1971−2000)

Category	Classification	Area (%)
Climate	Arid	21 %
	Semi-arid	34 %
	Dry	15 %
	Moist	9 %
	Wet	14 %
	Very wet	7 %
Season	Spring (AMJ[1])	13 %
	Summer (JAS[2])	1 %
	Fall (OND[3])	24 %
	Winter (JFM[4])	63 %
Subsurface Perm.	Low	40 %
	High	60 %
Terrain	Flat	7 %
	Transitional	63 %
	Mountain	30 %
Surface Perm.	Low	2 %
	High	98 %

[1]AMJ: April, May, and June
[2]JAS: July, August, and September
[3]OND: October, November, and December
[4]JFM: January, February, and March

https://doi.org/10.5194/hess-2019-638
Preprint. Discussion started: 23 January 2020

Hydrology and Earth System Sciences
Open Access
Discussions

Table 4. Hydrologic landscape characteristics of assessment units identified as vulnerable (having a vulnerability index greater than 7 on a scale of 10) for each metric.

	% Assessment units that share HL classification									
Vulnerability Parameter	Climate[1]		Seasonality[2]		Subsurface Perm.[3]		Terrain[4]		Surface perm.[3]	
Snow	75 %	D, M, or W	87 %	f or s	53 %	L	82 %	M	100 %	H
FMI	71 %	V or W	65 %	f	75 %	L	75 %	M	100 %	H
Seasonality	75 %	W or M	76 %	s	51 %	H	83 %	M	99 %	H
S'	92 %	A or S	79 %	w	75 %	H	87 %	M or T	99 %	H
ppt	72 %	D or S	79 %	f or w	71 %	H	97 %	M or T	98 %	H
tmean	70 %	D, S, or A	87 %	f or w	60 %	H	93 %	M or T	98 %	H
PET	70 %	D, S, or A	87 %	f or w	60 %	H	93 %	M or T	98 %	H

[1]A=arid, S=semiarid, D=dry, M=moist, W=wet
[2]f=fall, w=winter, s=spring
[3]L=low, H=high
[4]T=transitional, M=mountainous

https://doi.org/10.5194/hess-2019-638
Preprint. Discussion started: 23 January 2020

Appendix A

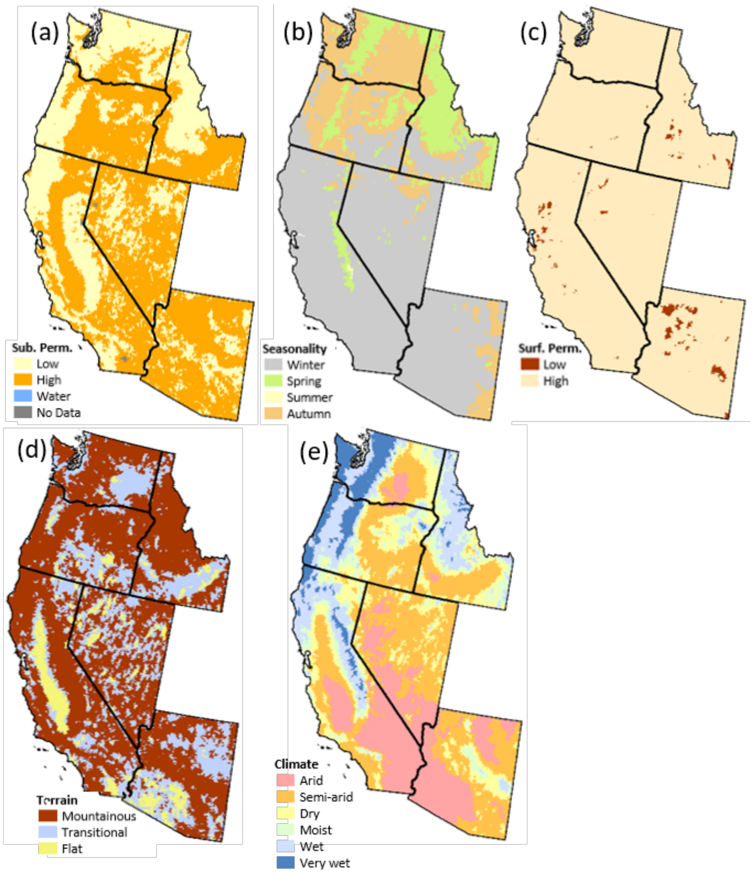

Figure A1. Hydrologic Landscape maps of Washington, Idaho, Oregon, California, Nevada, and Arizona were used in the HLVA analysis [(a) Subsurface Permeability, (b) Seasonality of precipitation surplus, (c). Surface permeability, (d) Climate, and (e) Terrain]. Notes: The seasonality map for the PNW has been updated from the original Leibowitz 2016 HL map, as we separated their winter seasonality into two seasons (winter and fall).

Hydrology and Earth System Sciences
Open Access
Discussions

Figure A2 (Plates 1–15)

Time series of average decadal temperature, precipitation, snow (April 1 snow water equivalent (mm), potential evapotranspiration (PET), available water (S'), FMI, and seasonality for specific locations identified in Fig. 1 and Table 2 in the western United States Dotted black line represents the 1971–2000 base period; the dashed red line connects the 2001–2010 value to the 2041–2070 climate projections. Note that Oregon, Washington, and Idaho locations are displayed first in alphabetical order and are followed by those of California, Nevada, and Arizona.

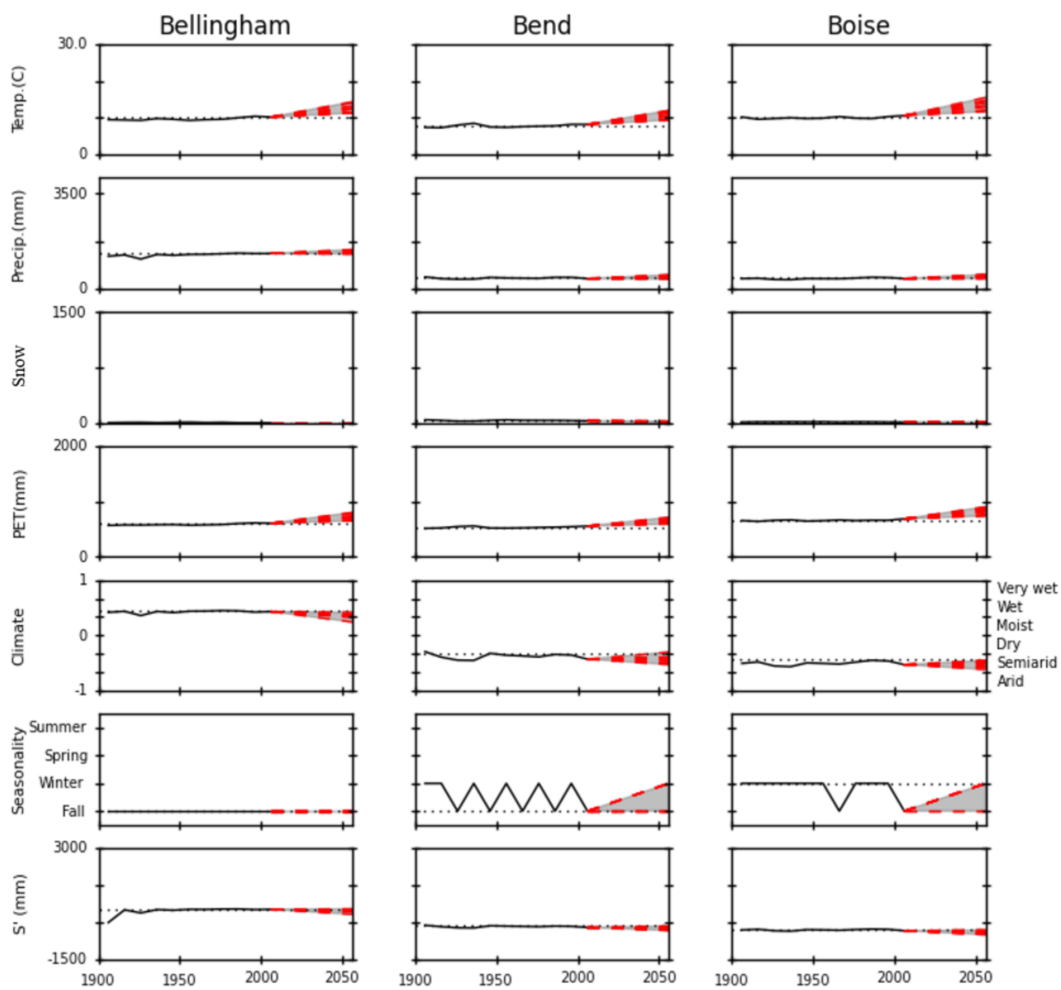

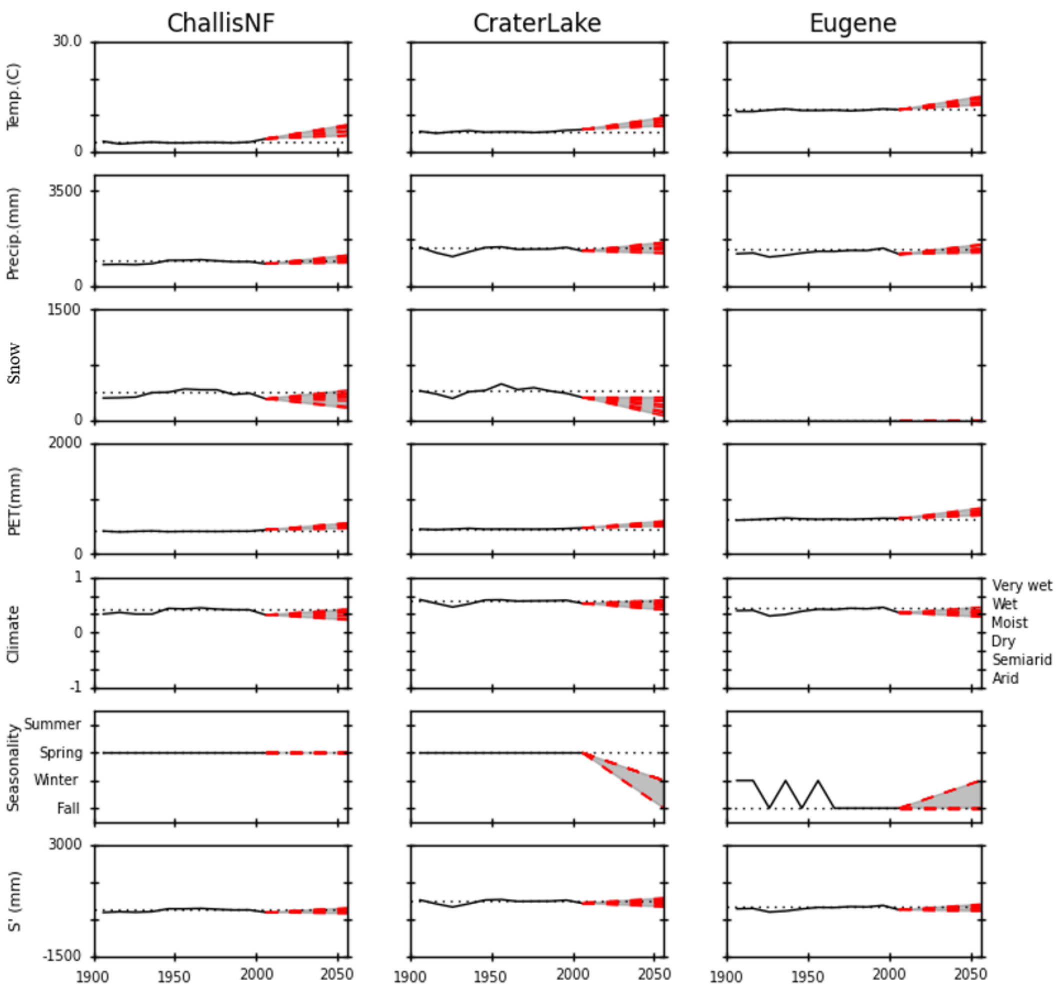
ChallisNF
CraterLake
Eugene
Temp.(C)
30.0
0
Precip.(mm)
3500
0
Snow
1500
0
PET(mm)
2000
0
Climate
1
0
-1
Very wet
Wet
Moist
Dry
Semiarid
Arid
Seasonality
Summer
Spring
Winter
Fall
S' (mm)
3000
-1500
1900
1950
2000
2050

817

https://doi.org/10.5194/hess-2019-638
Preprint. Discussion started: 23 January 2020

Hydrology and Earth System Sciences
Open Access
Discussions

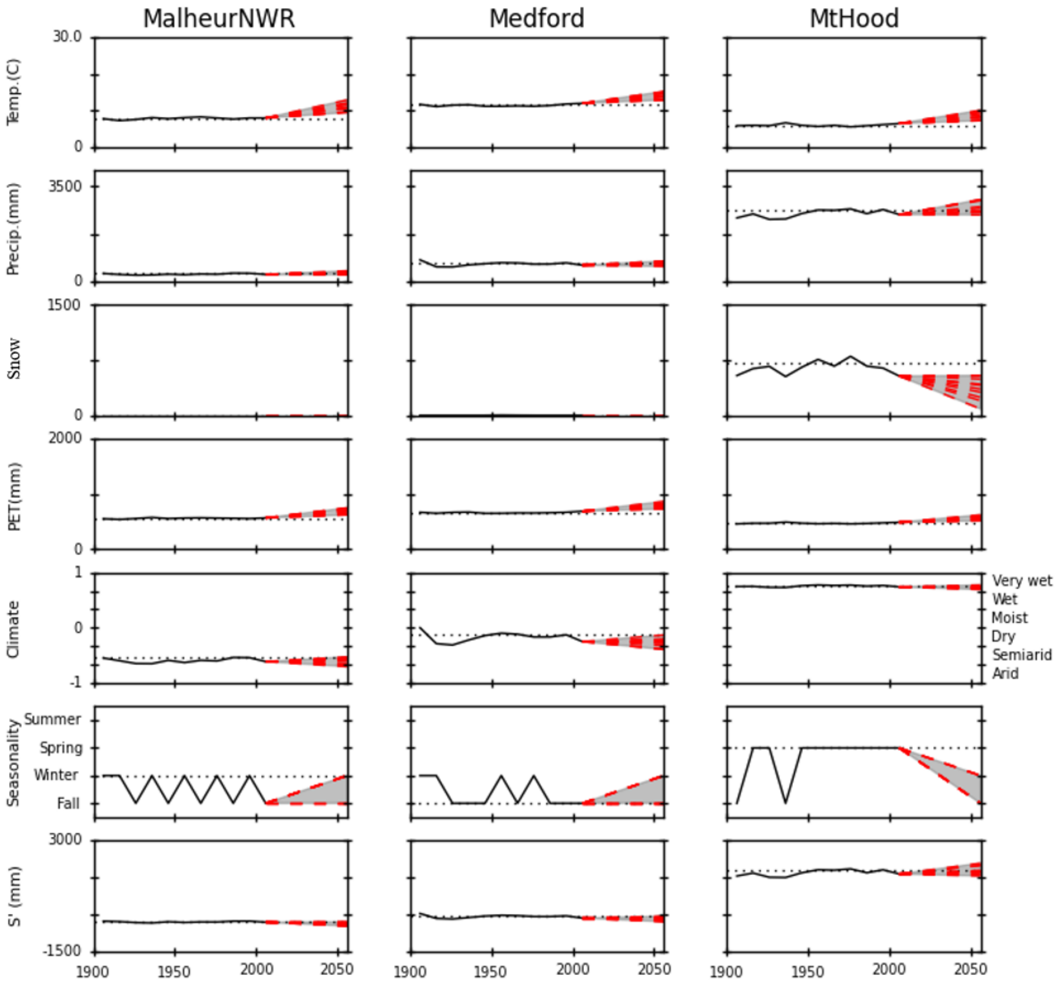

818

https://doi.org/10.5194/hess-2019-638
Preprint. Discussion started: 23 January 2020

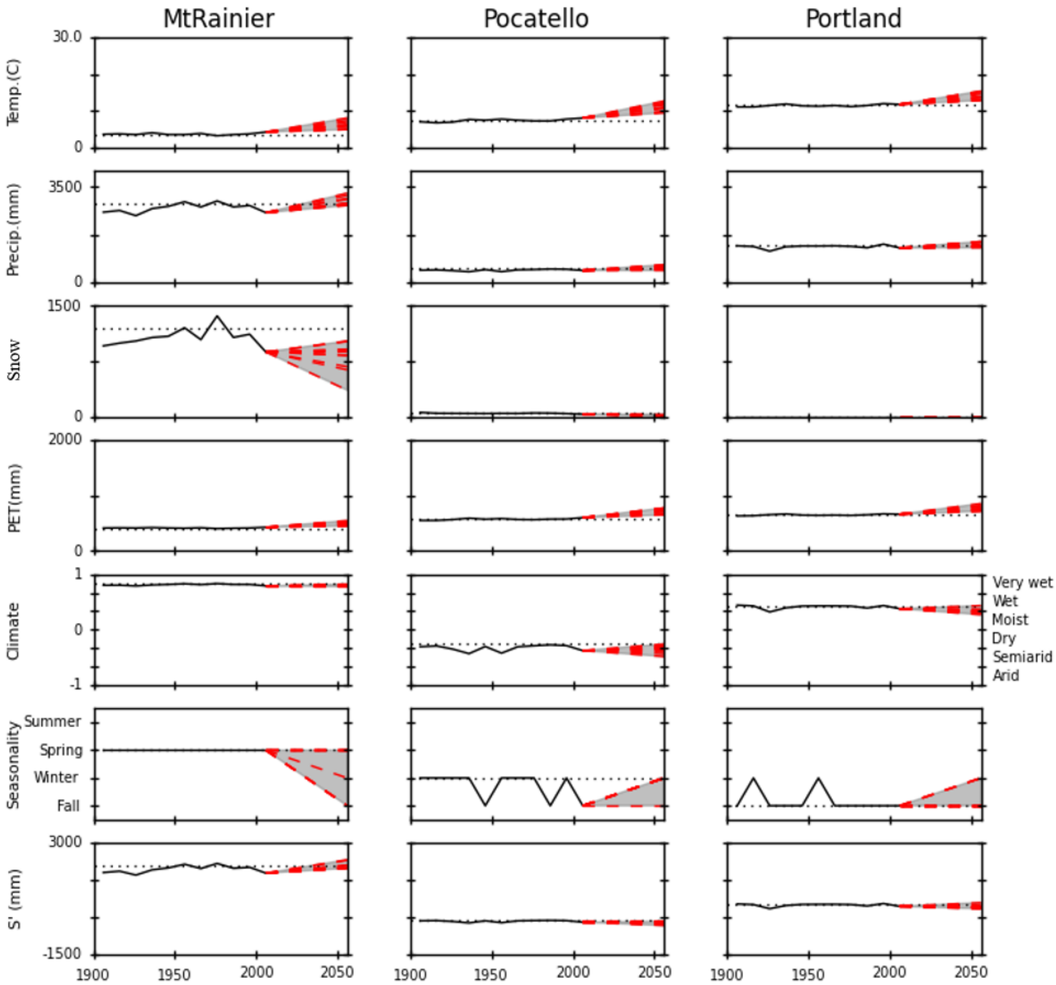

819

https://doi.org/10.5194/hess-2019-638
Preprint. Discussion started: 23 January 2020

Hydrology and Earth System Sciences
Open Access
Discussions

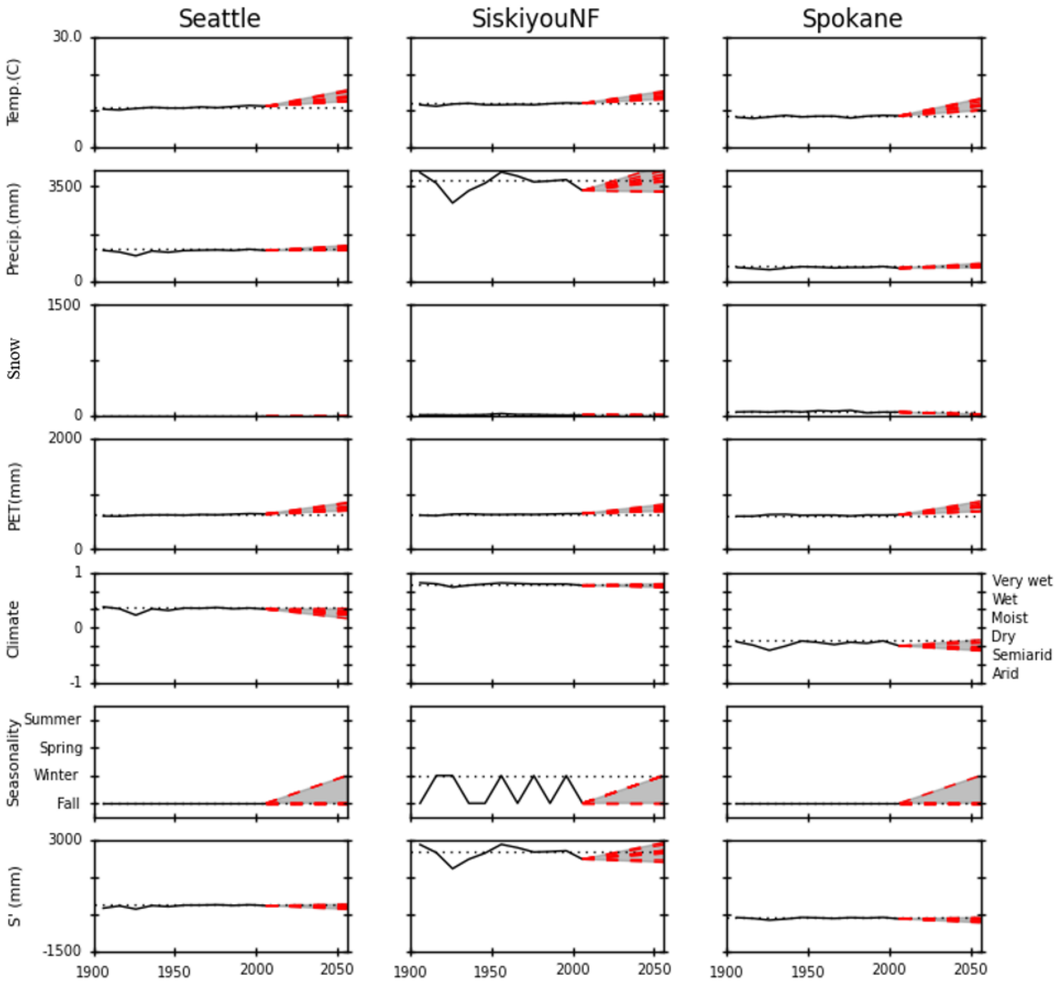

820

https://doi.org/10.5194/hess-2019-638
Preprint. Discussion started: 23 January 2020

Hydrology and Earth System Sciences
Discussions

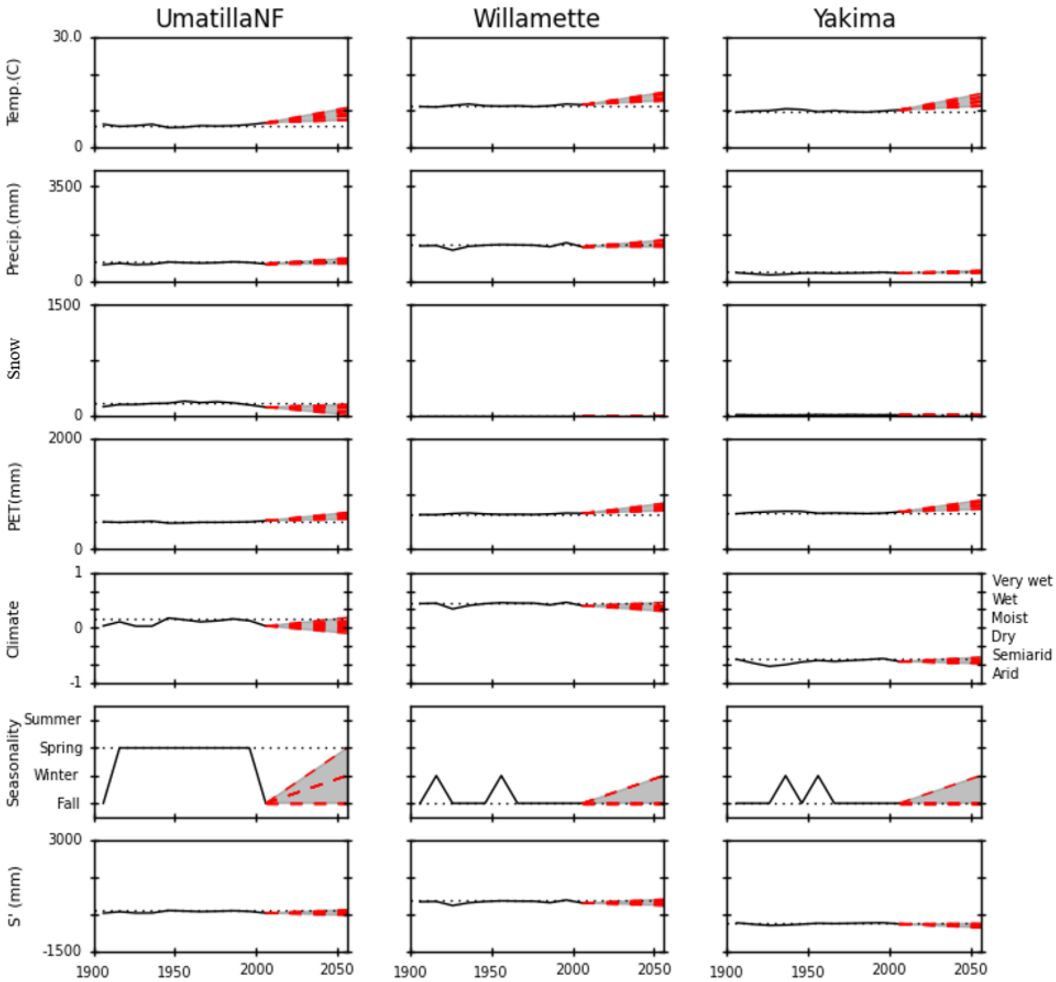

821

https://doi.org/10.5194/hess-2019-638
Preprint. Discussion started: 23 January 2020

Hydrology and Earth System Sciences
Open Access
Discussions

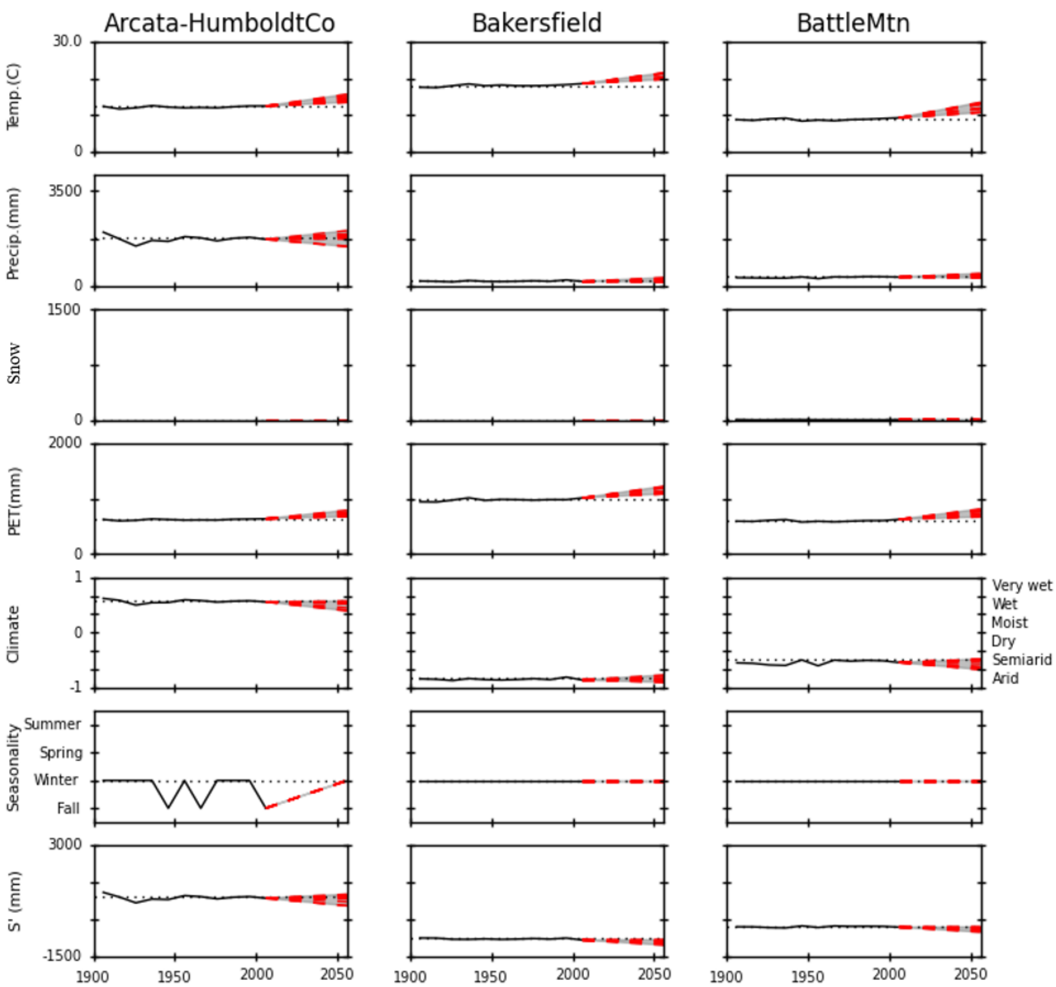

822

https://doi.org/10.5194/hess-2019-638
Preprint. Discussion started: 23 January 2020

Hydrology and Earth System Sciences
Open Access
Discussions

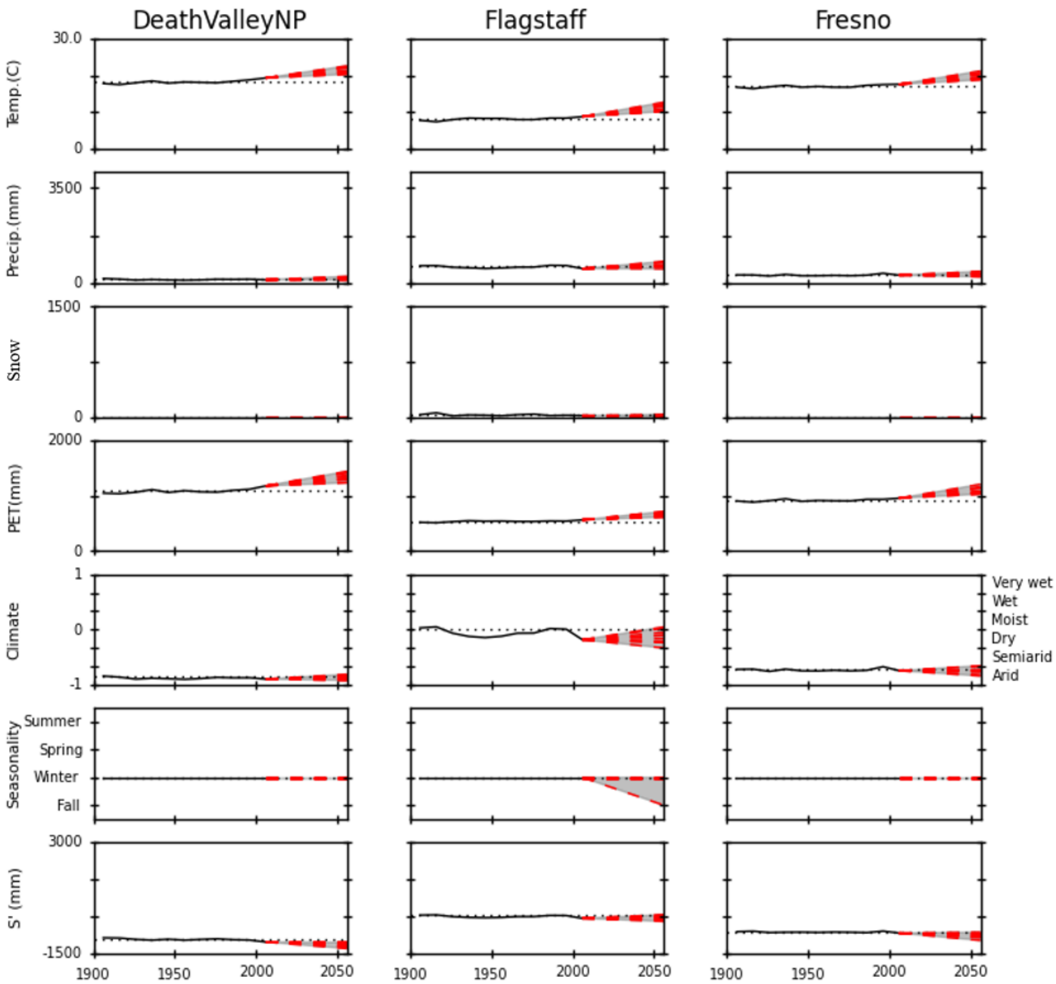

823

https://doi.org/10.5194/hess-2019-638
Preprint. Discussion started: 23 January 2020

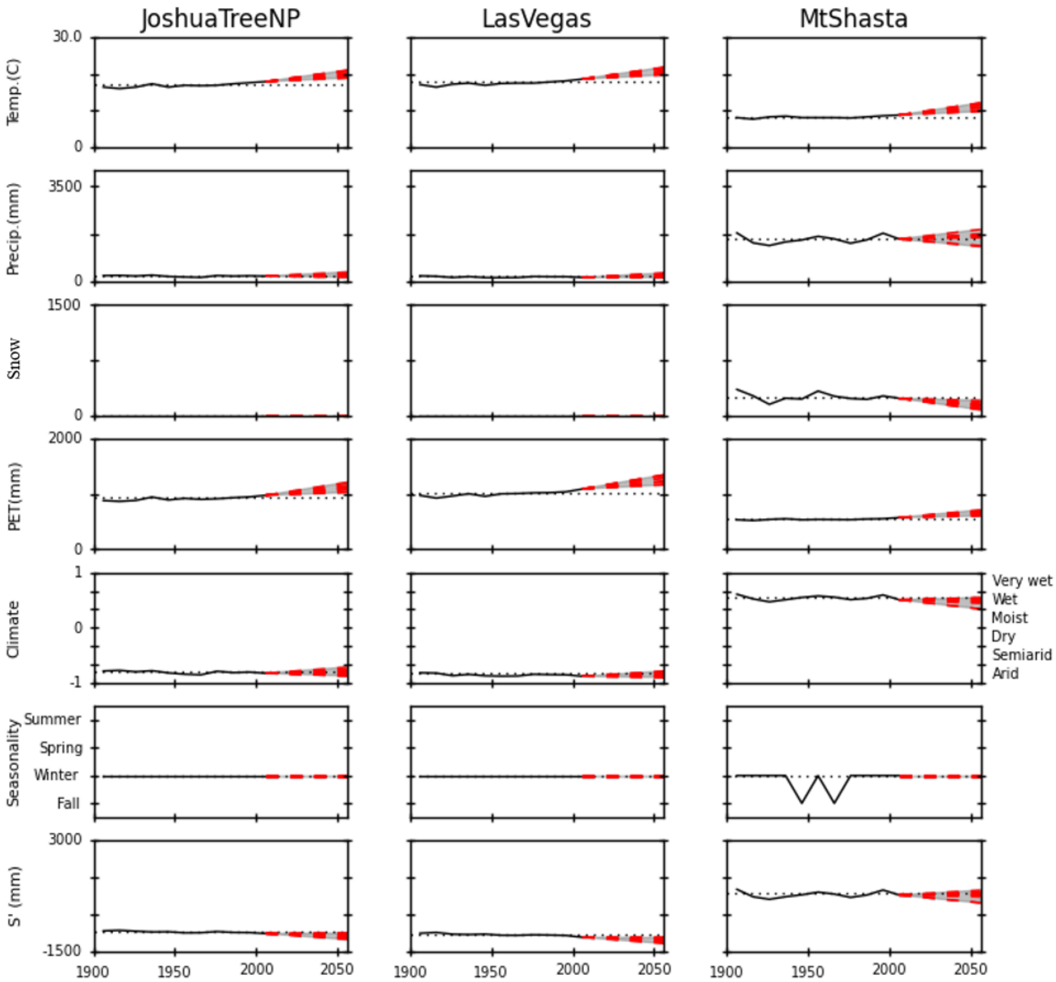

824

https://doi.org/10.5194/hess-2019-638
Preprint. Discussion started: 23 January 2020

Hydrology and Earth System Sciences
Open Access
Discussions

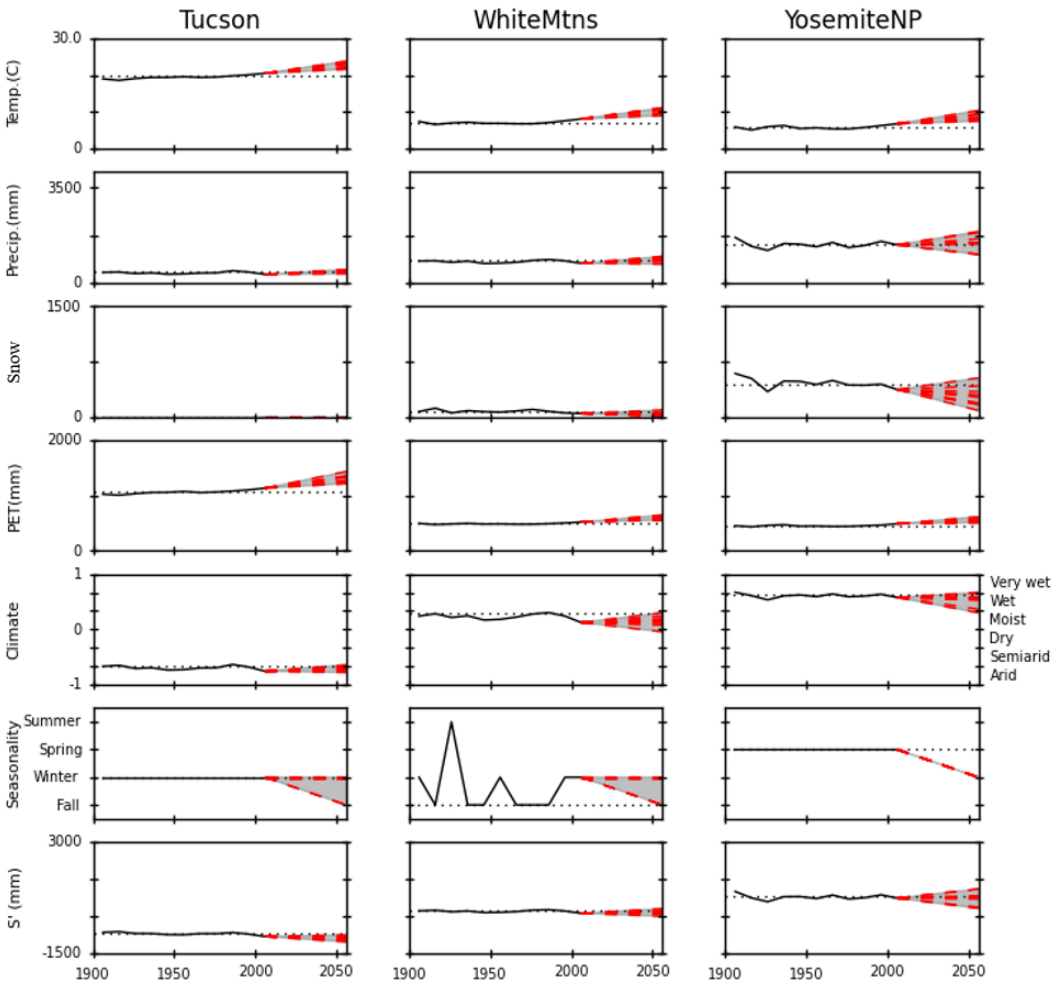

825

https://doi.org/10.5194/hess-2019-638
Preprint. Discussion started: 23 January 2020

Hydrology and Earth System Sciences
Discussions

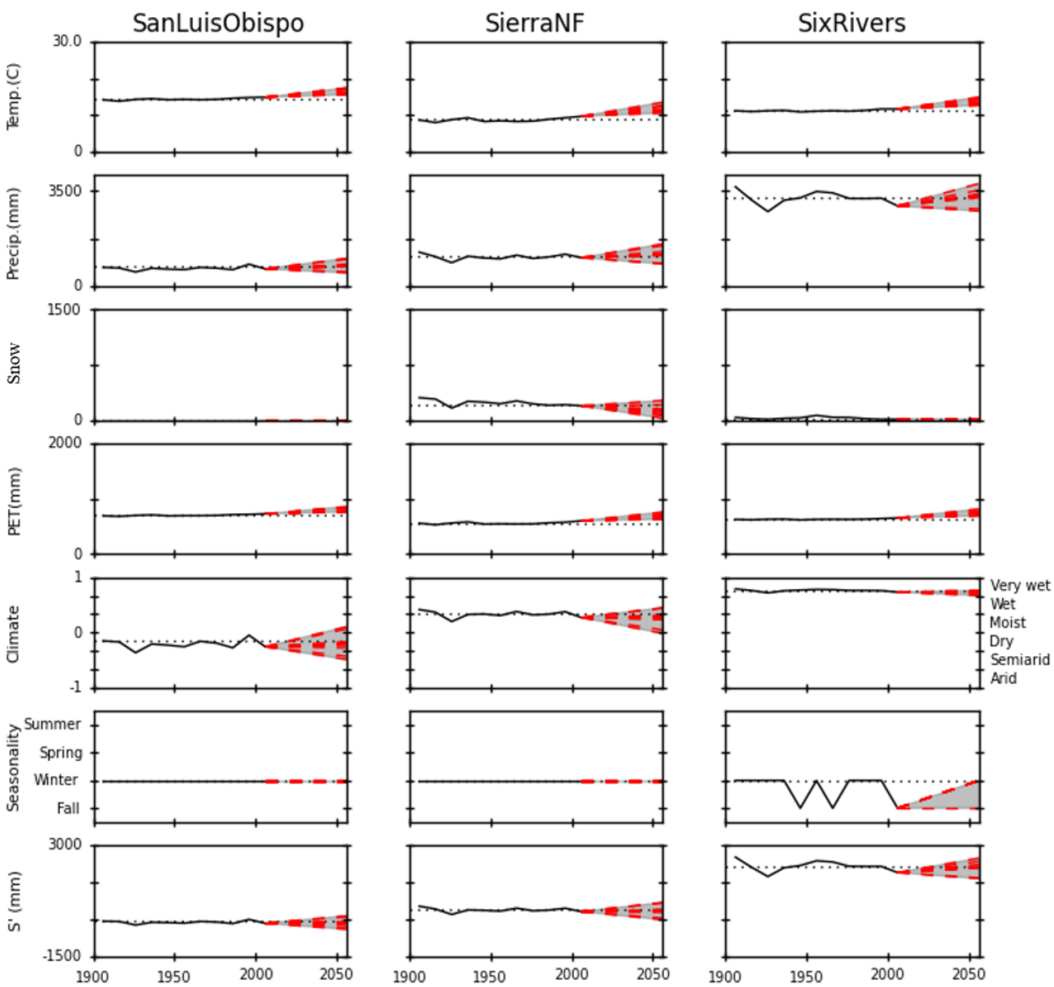

https://doi.org/10.5194/hess-2019-638
Preprint. Discussion started: 23 January 2020

Hydrology and Earth System Sciences
Open Access
Discussions

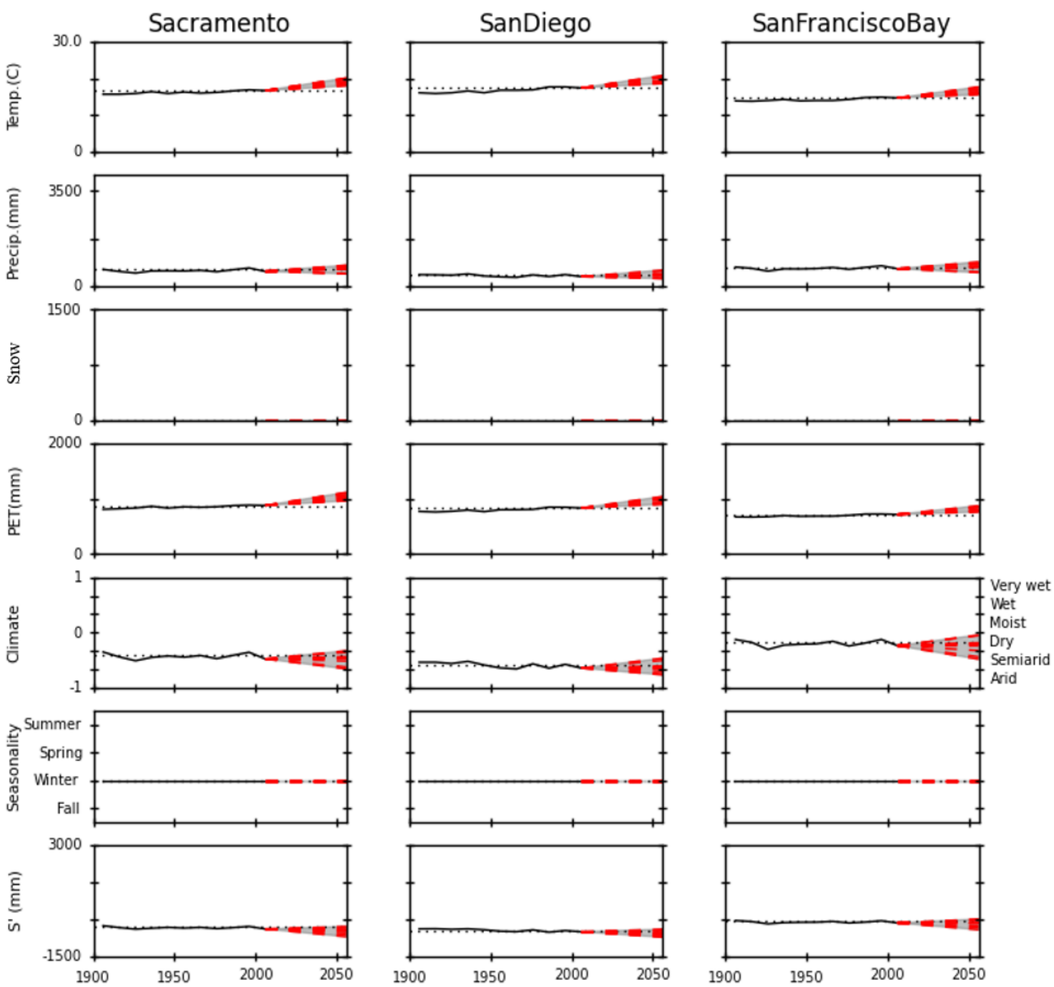

827

https://doi.org/10.5194/hess-2019-638
Preprint. Discussion started: 23 January 2020